ERROR-IN-VARIABLES FOR FAILURE CRITERIA APPLIED TO

THE NEAR-WELLBORE REGION

A Dissertation

by

ORLANDO ZAMBRANO MENDOZA

Submitted to the Office of Graduate Studies of
Texas A&M University
in partial fulfillment of the requirements for the degree of

DOCTOR OF PHILOSOPHY

May 2004

Major Subject: Petroleum Engineering

ERROR-IN-VARIABLES FOR FAILURE CRITERIA APPLIED

TO THE NEAR-WELLBORE REGION

A Dissertation

by

ORLANDO ZAMBRANO MENDOZA

Submitted to the Office of Graduate Studies of
Texas A&M University
in partial fulfillment of the requirements for the degree of

DOCTOR OF PHILOSOPHY

Approved as to style and content by:

Peter P. Valkó	James E. Russell
(Co-Chair of Committee)	(Co-Chair of Committee)
Luc T. Ikelle	Thomas A. Blasingame
(Member)	(Member)

Steve Holdich
(Head of Department)

May 2004

Major Subject: Petroleum Engineering

ABSTRACT

Error-in-Variables for Failure Criteria Applied to the Near-Wellbore Region.

(May 2004)

Orlando Zambrano Mendoza, B.S.; M.S., Zulia University (Venezuela)

Co-Chairs of Advisory Committee: Dr. Peter P. Valkó
Dr. James E. Russell

The development of a methodology to improve the parametric representation of the failure criteria used to characterize rock strength of a reservoir rock in the near-wellbore region is the focus of this study. We adopted a statistical method, so-called *error-in-variables* (EIV), to take into account experimental errors in all of the measured variables.

The proposed methodology is employed to obtain the parameters of the failure envelope (2D criteria) from experimental data in the following cases:

- When the experimental data are used directly to determine the failure envelope in the Mohr plane.

- When a failure envelope is first obtained in the principal-stress plane (σ_1, σ_3) and then transformed into the Mohr plane using Computer Algebra.

- When the presence of pore fluid requires the consideration of effective stresses.

- When the brittle-ductile transition requires special form of the envelope (cap models)

Using generalization of previously developed methods, we employed EIV methods to obtain the parameters of a failure surface in the principal-stress space (3D criteria).

The basic hypothesis of this work is that the EIV method provides a better representation of failure criteria than the previous methodology. The basic application of any failure criterion is to determine whether a certain stress state will or will not lead to failure. A parametric representation is considered better than another if the likelihood of obtaining the wrong answer is less than in the other case. Therefore, the best representation (within

a certain family of envelopes or surfaces) is the one minimizing the objective function, which is nothing else but the likelihood of this wrong answer.

To test the basic hypothesis of this work, I compared the objective function (likelihood of erroneous decision) calculated with parametric representations obtained by various methods. To achieve this I evaluated a well-documented, published set of experimental data, for which failure envelopes have been fitted by other methods.

This work is limited to the processing of data obtained in experiments conducted in homogenous, isotropic rock at isothermal conditions. Sedimentary rocks such as sandstone are the focus of this study because of their importance in near-wellbore reservoir rock stability problems. Nevertheless, the methodology developed in this work is not limited to this type of rock.

DEDICATION

Thanks to God and my Parents, Brothers and Sister who left in my soul the energy, endurance, and responsibility necessary to achieve challenges like this.

Maria, Leydiana Jakelin, and Juan Ernesto, this is for you all.

In memory of my little babies Lizana Corteza and Orlando Jose and my mother-in-love Josefina Govea.

ACKNOWLEDGEMENTS

TABLE OF CONTENTS

LIST OF TABLES

LIST OF FIGURES

CHAPTER I

INTRODUCTION

The purpose of this study is to develop a methodology to improve the parametric representation of the failure criteria used to characterize rock strength of a reservoir rock in the near-wellbore region. To understand this task, we must study the following parts: First, the use of failure criteria for reservoir rocks in the near-wellbore region; then the methods of obtaining parameters of the failure envelope or failure surface; and finally a review of the statistical method of error-in-variables.

1.1. Introduction

1.1.1. Failure criteria for reservoir rocks in the near-wellbore region

A failure criterion is used to delimit the boundary between failure and non-failure zones in the stress state. Its appropriate identification will be the key for modeling several complex processes associated with rock deformation and failure that may occur in the near-wellbore region of a hydrocarbon reservoir rock. In the process of identifying such a boundary, we need a parametric representation of the experimental data. Because of the scarcity of the experimental data even for a particular specimen of the reservoir rock, we need an appropriate statistical fitting of the measurements.

In the petroleum-engineering field, petrophysical properties such as porosity, permeability, saturation and capillary pressure are usually measured in the near-wellbore region to quantify the productive capability of a reservoir rock. Nevertheless, mechanical properties of the rock such as strength are needed to understand rock deformation and [1]failure processes. Strength defines the ability of the rock fabric to

This dissertation follows the style and format of the *SPE Reservoir Evaluation & Engineering.*

maintain cohesion; it is usually referred to as the rock's maximum load-bearing capacity. Failure has a connotation of loss of rock integrity or inability to perform a task such as keeping near borehole rock from sloughing into the hole. The concept of "failure" is not quite clear; even for a single rock specimen. A total loss of cohesion may or may not occur, depending upon the way it is loaded, expressed by stress-state components. In fact, a rock may fail through a combination of factors such as strain, stress, and loading path.

Stress/strain curves are useful when studying rock behavior under deformation. Since hydrocarbon-bearing reservoir rocks consist of the rock matrix and an interconnected pore network, rock formations can be considered as separate interfaces constituted of piece-wise continuous regions, where the medium parameters are discontinuous. However, the assumption of a continuous medium of the reservoir rock permits us to define stress (surface force per unit area) and strain (material deformation) tensors at a macroscopic scale. Some fundamental concepts arise from this definition. The classical view is that brittle fracture of a rock is a discrete event in which the failure of the rock occurs, without significant prior deformation and without warning, at a particular stress,[1] however, acoustic emissions always precede brittle fracture. The ductile state of a rock, on the other hand, defines the permanent deformation without losing its ability to resist load. The strength at the transition from brittle fracture to semi-brittle flow and from there to fully plastic flow is apparently a linear function of pressure, but the physical bases for this relation are still not well established.[2]

Many material models describe rock deformation by constitutive equations. The theory of linear elasticity assumes that a linear relation exist between stress and strain (and, consequently any process is reversible). Other theories have been developed to better consider the complex behavior of the reservoir rock (mainly when it is in compression). The theory of plasticity is of paramount importance when predicting the stress concentration around a wellbore or rock behavior during the reservoir depletion process. Moreover, the concept of elastoplasticity is used to define the material having elastic deformation until it reaches a yield point, after which plastic deformation occurs.

Several diagnostic tests are run in the laboratory to establish rock mechanical properties. The simplest is the uniaxial test; the indirect tensile strength (Brazilian test), which is used to obtain indirectly the rock tensile strength; the triaxial test, which considers the intermediate principal stress equal to one or the other of the extreme principal stresses, which is referred as the "true triaxial test"; or the polyaxial test, wherein all the three principal stresses are varied independently. A hollow cylinder provides the most common method of studying the strength of rock under a wide variety of unequal principal stresses.

Many factors affect rock strength. They may be grouped as rock type, including rock specimen and grain size (rock fabric); chemical reaction by the influence of water saturation and clay content; loading rate; stress and strain; a combination of confining pressure[3] and temperature; pore pressure; anisotropy, heterogeneities; deformation history; residual stress; and so on.

When considering the presence of pore fluids, the mechanical properties of porous rocks depend on both pore-fluid pressure and confining pressure according to an effective pressures law. The classical form of the effective pressure law, $p_e = p_c - p_p$, this relation can be used for many rock and soil types and physical properties.[4] In its more general form, can be expressed as $p_e = p_c - \alpha p_p$, where α is a constant rock type (referred to as Biot's constant). The Biot constant, α, can takes different values for different materials and it is always less than or equal to one.[5] The value of, α, is an indicator of the relative importance of pore-fluid pressure and confining pressure to the physical property under consideration.

Depending on the nature and magnitude of the applied stress as well as on rock properties, rocks fail under stress in different modes. Under applied stress, higher-porosity sedimentary rocks compact and lose porosity. The effective stress increases in the reservoir and may exceed the compressive strength of the rock matrix when hydrocarbons are withdrawal from the reservoir. The rock matrix collapses into the pore space in a mechanism known as "pore collapse."[6-7] Initially, lower effective stresses

cause little or no pore collapse, and deformation is recoverable. But as mean- effective stress increases, the reservoir undergoes unrecoverable pore collapse, accompanied by plastic deformation, which reduces porosity and permeability of the reservoir. The behavior of some porous rocks undergoes compaction, and elastoplastic constitutive relations can model pore collapse. But the behavior afterward is not perfectly plastic and a hardening rule is needed for a completed description. The behavior of porous sandstones undergoing pore collapse and compaction has been found to fit an approximately elliptical "cap model."[8]

A cap model consists of a failure envelope or surface for a perfectly plastic material response and an elliptic strain-hardening cap that extends isotropically about the hydrostatic axis.[9] The mechanical response in the elastic part of the curve is a function of the degree of sediment compaction prior to cementation and the level of cementation. The post-yield deformation, pore collapse, represents a gradual breakdown of the intergranular cementation, which is a transition from rock to sediment.[6]

A failure criterion is usually a relation between the principal effective stresses components and represents a limit for instability or failure. Several failure criteria have been proposed in the literature. Theoretical criteria per se provide an important basis of conceptual development and understanding, but their practical application is limited. For these reasons many empirical failure criteria have been developed from laboratory test experience.

Because of the physical limitation of the conventional triaxial compression and extension experimental set-up, empirical failure criteria are generally represented in two dimensions by a limited envelope in the stress-state plane neglecting the influence the intermediate principal stress. However, when the experimental equipment allow the intermediate principal stress to vary between σ_1 and σ_3, the empirical failure criteria are defined as a failure surface.

To obtain a failure envelope, a triaxial test should be performed at different confining pressures until failure is reached. Among various ways to represent the failure envelope, the classic approach is to plot either the effective stress or the stress at failure

for each test using a Mohr-circle representation. The resulting envelope is a locus separating stable from unstable conditions. Moreover, if the principal intermediate stress is considered having influence, which can be determined through a polyaxial or a hollow cylinder test, we can construct a failure surface as the boundary of stability.

Starting with the pioneering work of Balmer,[10] parametric equations have been proposed to represent the failure envelope in the Mohr's plane in terms of the principal stress. In this group we must include the empirical failure criteria equations.

This work does not propose to argue with any of those established failure criteria, having instead more interest in how to determine the optimum values of the parameters in the particular equations.

1.1.2. Methods of obtaining parameters of the failure envelope

Pincus[11] suggested a family of methods to construct the failure envelope piece-wise. To do this, he derived each segment envelope from a closed-form solution for two consecutives Mohr circles.

Balmer[10] and most researchers had been using the least-squares method to minimize the objective function when fitting the failure envelope. They emphasized that any least-squares method requires distinction between independent and dependent variables and requires that the former be known exactly.

Even with the great flexibility and simplicity of those proposed methods, we introduce reasons why those established methodologies may mislead us in the goal of minimizing the likelihood of making a wrong judgment (i.e. declaring a failure state as safe or a safe state as failure).

1.1.3. The statistical method of error-in-variables

In the least squares approach to parameter estimation, a distinction is made between dependent and independent variables, with the assumption that there are no measurement errors in the independent variable. The presence of error in all the variables is taken into account in the error-in-variable (EIV) approach.

In the case of triaxial test data, both measured quantities-the axial and lateral stresses and any new variable derived for them-are corrupted by error. Therefore, there is no justification to assume that any variables of them has been measured without error. This poses an inherent limitation on least-squares-based methods of determining the failure envelope.

On the other hand, even if the piece-wise envelope construction provides great flexibility, it has some drawbacks:

- The resulting envelope is not smoothing (differentiable) at the intersecting point of two segments.
- Construction of the segments requires pre-processing to create "average circles," which is difficult to justify from a statistical point of view.

For these reasons, we employ a new methodology to improve obtaining the parametric representation of the failure envelope in the Mohr plane, taking into account measurement errors in all the variables. To accomplish this task, we used the statistical method of error-in-variables (EIV).

Additionally, we extended the use of this methodology to fit the failure criteria in the principal stress plane and space as well as in the identification of the brittle/ductile transition and pore collapse. This allowed us to calculate either the yield envelope or the yield surface in the principal effective stresses plane or space respectively.

1.2. Statement of the problem

In the characterization of the mechanical behavior of rock, parametric representation of the rock-strength failure criteria is one of the basic tasks.

Several methods have been proposed for envelope fitting. A review shows that all of the available methods ignore the fact that all measured variables may be corrupted by error. we suggest an improvement in obtaining the parametric representation of the failure envelope, taking into account measurement errors in all the variables, with statistical method called error-in-variables (EIV). Our methodology extends to obtain the parametric representation of the failure surface in the principal-stress space.

The basic hypothesis of this work is that the EIV method provides a better representation of the failure envelope than the previously used methodology. To understand what we mean by better representation of the failure criteria, we have to consider how it is applied. The basic application of any envelope is to answer the question whether a certain stress state will lead to failure or not. A parametric representation is considered better than another if the likelihood of obtaining the wrong answer is less than in the other case. Therefore, the best representation (within a certain family of envelopes or surfaces) is the one minimizing the objective function, which is nothing else but the likelihood of this wrong answer.

To test the basic hypothesis of this work, we compared the objective function (likelihood of erroneous decision) calculated with parametric representations obtained by various methods. For this purpose we evaluated a well-documented, published set of experimental data, for which envelopes have been fitted by other methods. Then we extended the methodology to 3D.

This work is restricted to the processing of data obtained in experiments conducted in homogenous, isotropic rock at isothermal conditions. Sedimentary rocks like sandstone are the focus of this study because of their importance in near-wellbore reservoir rock stability problems. Nevertheless, the developed methodology is not limited to this type of rock.

1.3. Research objectives

The proposed research aimes:

To employ the EIV method for obtaining the parameters of the failure envelope (2D criteria) from experimental data for the following cases:

- when the experimental data are used directly to determine the failure envelope in the Mohr plane.
- when a failure envelope is first obtained in the principal stress plane (σ_1, σ_3) and then transformed into the Mohr plane using Computer Algebra.
- when the presence of pore fluid requires the consideration of effective stresses.
- when the brittle-ductile transition requires special form of the envelope (cap models).

We employed EIV methods for obtaining the parameters of a failure surface (3D criteria) through generalization of the previously developed methods.

To simplify the application of this methodology, we developed a computer code and used published data. The main goal of this research was to demonstrate an improvement in how the fitted failure envelope can predict stability, using a well-documented set of experimental data.[12-14] In addition, a new approach is introduced for the case where the experimental data allow us to define the failure surface. I anticipate that this research will serve as the base for future development; mainly focusing in the analysis of some complex near-wellbore rock stability problems like subsidence and/or sand production, among others.

1.4. Methodology

To achieve these objectives and test the hypothesis, we developed a curve-fitting methodology based on the statistical method of error-in-variables (EIV), which considers all the measured variables having experimental error. We used triaxial and

polyaxial test data reported from previous work to verify and illustrate the validity of our proposed methodology. Details of the methodology used to fit the failure envelope and failure surface are presented in Chapters III and IV respectively. To simplify the application of our proposed methodology we developed a computer code. The derivations of the parametric representation of the failure envelope and failure surface are shown in Appendix A and B respectively. A stepwise procedure for the estimation of the parametric representation of the failure criteria is presented in Appendix C.

CHAPTER II

LITERATURE REVIEW

2.1. Introduction

This chapter presents a review of the technical literature relevant to our methodology. The review of literature is divided into three main sections in accordance with the main objective of this study: rock mechanics failure criteria, existing methods to obtain the parameters, and the statistical method of error-in-variables.

2.2. Rock mechanics failure criteria

The simplest and best-known rock-failure criterion is the Mohr-Coulomb criterion, also known as Coulomb-Navier criterion. It consists of a linear envelope touching all Mohr's circles representing a critical combination of principal stresses. Stated in terms of normal and shear stresses on the plane represented by the point of a Mohr's circle with the envelope,

$$\tau_p = \tau_o + \sigma \tan \phi \quad \text{..} \quad \text{(2-1)}$$

ϕ is called the angle of internal friction, for like a friction angle between sliding surfaces, it describes the rate of peak strength with normal stress; τ_p is the peak shear stress, or shear strength; and τ_o is the cohesive strength.

Mohr proposed that when shear failure takes place across a plane, the normal stress σ and the shear stress τ across this plane are related by a functional characteristic of the material:

$$|\tau| = f(\sigma) \dots\dots\dots\dots\dots\dots\dots\dots\dots\dots\dots\dots\dots\dots\dots\dots \quad (2\text{-}2)$$

Eq. 2-2 will be represented by a curve in the σ-τ plane as shown in **Fig. 2-1.** Considering **Fig. 2-1.a** for a rock specimen subjected to principal failure stresses, σ_1 and σ_3, the normal and shear stresses on an inclined failure plane are.

$$\sigma = \frac{\sigma_1 + \sigma_3}{2} - \frac{\sigma_1 - \sigma_3}{2}\cos 2\beta \dots\dots\dots\dots\dots\dots\dots\dots\dots\dots\dots\dots\dots..(2\text{-}3)$$

and

$$\tau = \frac{\sigma_1 - \sigma_3}{2}\sin 2\beta \,,\dots\dots\dots\dots\dots\dots\dots\dots\dots\dots\dots\dots\dots\dots\dots..\dots\dots.(2\text{-}4)$$

where β is the angle between the direction of σ_1 and the inclined plane. A Mohr circle for various orientations of the plane can represent Eqs.2-3 and 2-4. **Fig. 2-1.b.** shows the angle β when failure passes through the plane and the corresponding magnitudes of σ and τ on the plane. Then for every pair (σ_1, σ_3) producing failure there will be a circle, producing a family of circles. The curve enveloping these circles is the Mohr envelope. Thus, the failure criteria represented in implicit form as

$$f(\sigma_1, \sigma_3) = 0 \,,\dots\dots\dots\dots\dots\dots\dots\dots\dots\dots\dots\dots\dots\dots\dots\dots\dots..\dots\dots.(2\text{-}5)$$

in terms of the principal stresses can be represented by a Mohr envelope in (σ, τ) coordinates. **Fig. 2-1.c** shows the two representations of a failure criterion:

- o In the principal stress plane having as intercepts the uniaxial compression σ_c, and the tensile strength σ_t.
- o In the Mohr plane having as intercepts the shear strength τ_s and the tensile strength σ_t.

Griffith[12] proposed a hypothesis that considered that a fracture is caused by stress concentration at the tips of minute cracks. For true triaxial or polyaxial criteria, see also the proposed Modified Wiebols and Cook,[16] Modified Lade,[17] circumscribed and inscribed Ducker and Prager,[18] and Murrel.[19]

Several empirical criteria have evolved over the past five decades in an attempt to simulate triaxial behavior of in-situ rock specimens. Most of the equations were proposed for a few particular rock types in each case using a limited number of data[20] until 1980, when Hoek and Brown[21] developed a new failure equation and fitted it comprehensively to different rock types. Some of the equations were given only in the compression regions of the failure criterion and in fact do not exist in the tensile quadrant; this implies a limitation since a failure criterion should exist both in the tensile and compressive region to be comprehensive enough.[22] Sheorey[23] shows a list of the most relevant failure equations not only when considering that the intermediate principal stress does not affect failure, but also in the case considering the influence of the intermediate principal stress.

The Hoek-Brown[21] empirical failure criterion was developed in the early 1980s. In common with most of the empirical failure criteria, it was formulated in terms of σ_1 and σ_3 and independent of σ_2. It has been a common practice for researchers fitting empirical failure criterion to exclude results thought to exhibit ductile behavior; Hoek and Brown[21] and Shoerey[23] among others have adopted this approach. In general these researchers have adopted the brittle/ductile transition suggested by Mogi[24] of $\sigma_1 = 3.4\sigma_3$. The exclusion of ductile data would be appropriate if only brittle behaviors were of interest, the boundaries were clear, and the failure criteria were disjoint across the transition. In the case of a criterion based only on Griffith's[15] theory, exclusion of the ductile tests would be appropriate. Evans *et al.*[2] show that the transition is not well defined for all rocks and certainly occurs over a wide range of stresses. That research shows that the failure envelope is not necessarily disjointed at the brittle/ductile transition. Thus, an appropriate criterion can model strength on both sides of the
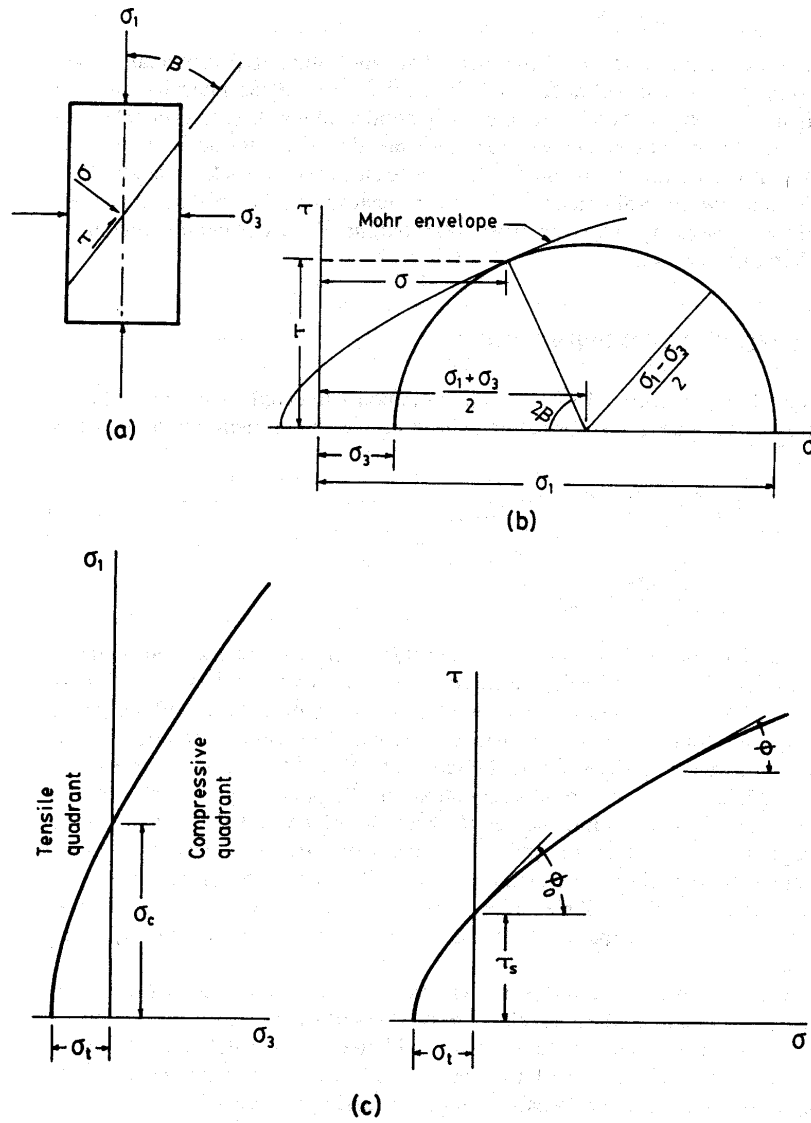
Fig. 2-1- (a) Stresses on an inclined plane in a rock specimen subjected to principal stresses represented by (b) Mohr circle and envelope and (c) two versions of a failure criterion.[23]

transition. In our case, we proposed a methodology to treat the failure envelope without a disjoint in the brittle/ductile transition. In 1988 Pan and Hudson[25] reviewed several criteria which include the influence of principal stress σ_2 and proposing a 3D variation of the Hoek-Brown criterion. Wang and Kemeny[26] made a modification of Beiniawiski's equation based on hollow-cylinder test results of three rock types. Such criteria provide a failure or failure surface in the principal-stress space.

Since we are dealing with a saturated porous medium, we must introduce the concept of poroelasticity to define the deviatoric or effective stress. Terzagui[4] was the first who considered the influence of pore fluid on the quasistatic deformation of soils in his one-dimensional consolidation model. Biot[27] later developed a linear theory of poroelasticity, which dealt with the relationships between pore fluid pressure and both compression and dilation of the rock, assuming a solid that is linear, elastic, and isotropic.

Adopting the Mohr-Coulomb criterion[3,28] the critical shear stress at failure (fracture) for a fluid-saturated rock with $\alpha = 1$ Eq. 2-1 can be expressed as:

$$\tau_p = C_o + (\sigma - p_p)\tan\phi \dots\dots\dots\dots\dots\dots\dots\dots\dots\dots\dots\dots\dots\dots\dots\dots(2\text{-}6)$$

Moreover, rocks fail under stress in different modes depending on the nature and magnitude of the applied stress and on the properties of the rock itself. Higher-porosity sedimentary rocks are found to compact and lose porosity under applied stress. When fluids are produced, the effective stress increases in the reservoir and may exceed the compressive strength of the rock matrix. The rock matrix collapses into the pore space in a mechanism known as "pore collapse."[6-7] Initially, lower effective stresses cause little or no pore collapse, and deformation is recoverable. But as effective stress increases, the reservoir undergoes unrecoverable pore collapse, accompanied by elastic deformation, which reduces porosity and permeability of the reservoir. The behavior of some porous

rocks undergoes compaction and elastoplastic constitutive relations can model pore collapse. But the behavior afterward is not perfectly plastic and a hardening rule is

needed for a completed description. The behavior of porous sandstones undergoing pore collapse and compaction has been found to fit an approximately elliptical "cap model."[8]

A cap model consists of a failure surface for a perfectly plastic material response and an elliptic strain-hardening cap that extends isotropically about the hydrostatic axis.[9]

The mechanical response in the elastic part of the curve is a function of the degree of sediment compaction prior to cementation and the level of cementation. The post-yield deformation, pore collapse, represents a gradual breakdown of the intergranular cementation, which is a transition from rock to sediment.[6]

This work does not propose to refute or argue about the established rock-failure criteria methods. Instead, some of them will be considered to be the bases in the development of our methodology, as is the case of Mohr failure criterion as well as Balmer[10] method.

2.3. Existing methods to obtain the parameters of failure envelope

Using a published ASTM interlaboratory study of the precision of rock-properties test methods, Pincus[11] presented closed-form solutions for rock-strength failure envelopes for a pair of Mohr stress circles in a loading series. Linear, parabolic, and hyperbolic envelopes were used to evaluate the coordinates of the envelopes' points of tangency with the stress circles. In addition, for a series of three or more circles, he used four types of least-squares (linear, second-order polynomial, parabolic, and hyperbolic) as well as three types of cubic-spline curves to fit the point of tangency.

Finding an exact equation for Mohr's envelope corresponding to a failure criterion defined in terms of the principal stresses is not always possible. Balmer[10] has given a simple method to determine the normal and shear stresses (σ, τ) for any given values of σ_1, σ_3. The family of Mohr circles can be defined by the general equation:

$$\left(\sigma - \left(\frac{\sigma_1 + \sigma_3}{2}\right)\right)^2 + \tau^2 = \left(\frac{\sigma_1 - \sigma_3}{2}\right)^2 \quad \dots\dots\dots\dots\dots\dots\dots\dots\dots\text{(2-7)}$$

and

$$\sigma = \sigma_3 + \frac{\sigma_1 - \sigma_3}{\dfrac{d\sigma_1}{d\sigma_3} + 1},\dots\dots\dots\dots\dots\dots\dots\dots\dots\dots\dots\dots\dots\dots\dots\dots\dots\dots\dots(2\text{-}8)$$

$$\tau = \frac{\sigma_1 - \sigma_3}{\dfrac{d\sigma_1}{d\sigma_3} + 1}\sqrt{\dfrac{d\sigma_1}{d\sigma_3}}\ \dots\dots\dots\dots\dots\dots\dots\dots\dots\dots\dots\dots\dots\dots\dots\dots\dots(2\text{-}9)$$

Eqs. 2-8 and 2-9 are important and provided the basis for further deductions, such as the Hoek and Brown method.[21] The equations are perfectly general and apply to a linear or a curvilinear envelope. To fit the envelope, Balmer used the least-squares statistical method; however, he stated that methods other than least-squares could be used for fitting the envelope if desired.

The method of least squares is very widely adopted in fitting models to experimental data, but we should emphasize that it requires the distinction between independent and dependent variables, requiring that the former is known exactly.

Even with the great flexibility and simplicity of those proposed methods, the established methodologies may mislead us in the purpose to minimize the likelihood of making a wrong judgment (i.e. declaring a state of stress as suspect to failure state as safe or vice versa). For this reason, we introduce a methodology that considers that all the measurements are corrupted.

2.4. The statistical method of error-in-variables

The presence of measurement errors in both system variables x and y is taken into account in the EIV approach, when formulating the objective function of the parameter estimation problem. The model is written in implicit form,

$$f(\hat{x}, \hat{y}, \underline{\theta}) = 0 \text{,} \ldots\ldots\ldots\ldots\ldots\ldots\ldots\ldots\ldots\ldots\ldots\ldots\ldots\ldots\ldots\ldots\text{(2-10)}$$

where $\underline{\theta}$ is the vector of unknown parameters, $\hat{x}$ and $\hat{y}$ are "corrected" state variables. If we denote the measurements by x_i and y_i (i = 1,2, …. n) and their corrected (or reconciled) value by $\hat{x}_i$ and $\hat{y}_i$, then our goal is to find the optimum parameters at which the sum of necessary corrections squared:

$$J = \sum_{i=1}^{n} d_{p_i}^2 \ \ldots\ldots\ldots\ldots\ldots\ldots\ldots\ldots\ldots\ldots\ldots\ldots\ldots\ldots\ldots\text{(2-11)}$$

is minimum, where

$$d_{p_i}^2 = \left(\hat{x}_i - x_i\right)^2 + \left(\hat{y}_i - y_i\right)^2 \ \ldots\ldots\ldots\ldots\ldots\ldots\ldots\ldots\ldots\ldots\ldots\ldots\text{(2-12)}$$

As shown in Fig. 2-2, the correction corresponds to the true distance of the point from the envelope, while in traditional least-squares only the vertical distance (d_{iLS}) is considered. In the EIV method the reconcile point on the envelope is obtained from the concept of shortest distance, which is given by a perpendicular line connecting the measured point with the tangential vector on the curve.

Because the variables x and y are affected by experimental error, they should contain the same units. If there is the case when each coordinate has different units we can use the concept of relative distance.

EIV methods have gained popularity in some engineering fields. Deming[29] was the first to formulate the general EIV problem. His primary concern was to obtain
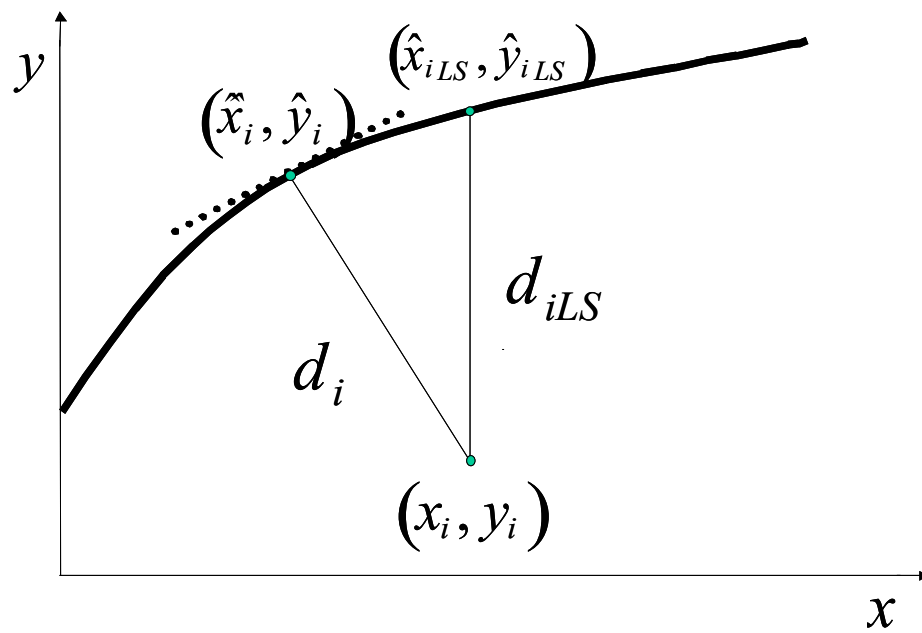
Figure. 2-2- Geometric representation of the distance using least-squares (d_{iLS}) and error-in-variables (d_i) approaches.

approximate solutions, suitable for hand calculations. Until the beginning of the 1970s, exact solutions were proposed by other researchers,[30-33] concerning straight lines or higher-order polynomials. Later on, Britt and Luecke[34] suggested a general algorithm based on the concept of Lagrange multipliers. Peneloux *et al.*[35] and Reilly and Patino-Leal[36] provided computational improvements. Schwetlick and Tiller[37] and Valkó and Vajda[38] separated the parameter estimation and data reconciliation steps. Liebman and Edgar[39] and Liebman *et al.*[40] investigated the use of nonlinear parameter-estimation (NLP) techniques, not only in the parameter estimation, but also in the data-reconciliation step. Esposito and Floudas[41] applied global optimization to avoid being trapped in a local minimum.

CHAPTER III

FITTING PARAMETRIC MODELS IN 2D

3.1. Introduction

In this chapter, we present the application of the statistics-based method of error-in-variables (EIV) to fit the failure envelope in 2D. To achieve this task, we partitioned the application of the EIV methodology into four main parts. First, since the Mohr failure criterion has been widely used to obtain the parametric representation of the failure envelope in 2D, we deal with the case where the failure envelope fits directly into the Mohr plane. Second, from the triaxial data, we represent the failure envelope in the principal-stress state plane and then transform the resulting envelope into the Mohr plane using Computer Algebra. Third, considering the poroelastic effect for porous sedimentary reservoir rock, we fit the failure envelope in the principal effective stress plane in terms of the mean effective stress and the equivalent stress. Finally, introducing the pore collapse effect for highly porous sedimentary rocks, we describe brittle/ductile transition behavior in the yield envelope, which has been found to fit an approximately elliptical "cap model."[9]

In this study, we used a well-documented set of data[12-14, 23, 42-43, 44] to test the hypothesis that the EIV method that considers all the variables to be influenced by experimental error provides a better representation of the failure envelope than the previously proposed methodology. We must recall that the basic application of any envelope is to determine whether a certain stress state will lead to failure or not. Therefore, one parametric representation of the envelope is considered better than another if the likelihood of obtaining the wrong answer is less than in the other case.

To test the proposed hypothesis, we compare the EIV methodology with the closed-form solution proposed by Pincus,[11] fitting the failure envelope directly in the

Mohr plane. The parametric representation of the failure envelope using the EIV method in the principal stress plane is compared with the parametric representation of such an envelope using traditional least-squares, which requires a distinction between independent and dependent variables. We establish and verify that the EIV method leads to a lower value for the objective function than the least squares method, we extend the application to special models suitable for describing the brittle/ductile transition. We restrict this work to the processing of data obtained in triaxial experiments conducted in homogenous, isotropic rock at isothermal conditions. Sedimentary rocks like sandstone are the focus of this study because of their importance in near-wellbore, reservoir-rock stability problems; however, the proposed methodology is not restricted to this type of rock, as we show when fitting the failure envelope in the Mohr plane.

3.2.   Fitting failure envelope directly in the Mohr plane.

3.2.1. Introduction

In the near-wellbore region of a reservoir, we encounter phenomena of rock instability including subsidence, borehole stability and sanding propensity. A failure envelope, which separates stable and unstable zones of the stress state, is the key for modeling such phenomena. An appropriate closed-form representation of this envelope is of great importance in practical applications. Because of the physical limitations of the experimental set-up, a failure criterion is expressed in terms of the maximum (σ_1) and minimum (σ_3) principal stresses. In this case, the criterion may be represented by the equation, Sheorey[23]:

$$g(\sigma_1, \sigma_3) = 0 \qquad\qquad (3\text{-}1)$$

where $\sigma_1 > \sigma_2 = \sigma_3$

For every stress state (σ_1, σ_3), producing a failure during the triaxial failure experiments, a Mohr circle may be drawn on the σ, τ plane by recognizing that the center of the circle is $\dfrac{(\sigma_1 + \sigma_3)}{2}$ and the radius is $\dfrac{(\sigma_1 - \sigma_3)}{2}$.

$$\left(\sigma - \frac{\sigma_1 + \sigma_3}{2}\right)^2 + \tau^2 = \left(\frac{\sigma_1 - \sigma_3}{2}\right)^2 \quad \text{..(3-2)}$$

The failure envelope is defined as the curve enveloping all these circles. The equation of the failure envelope may be represented as

$$f(\sigma, \tau) = 0 \quad \text{..(3-3)}$$

Zambrano-Mendoza, Valkó and Russell[45] state that because of the experimental errors and stochastic variations in the rock itself, there is no guarantee of creating a deterministic curve to represent the failure envelope. Rather, the problem consists of selecting a suitable algebraic form of Eq. (3-3) and determining its unknown parameters from a suitable criterion related to minimizing possible false judgment of failure in future applications.

Several approaches have been suggested in the literature, most often based on the method of least squares, starting with the pioneering work of Balmer. [10]

However, Zambrano-Mendoza *et al.*[45] emphasize that the method of least squares requires distinction between independent and dependent variables, requiring that the former be known exactly. This poses an inherent limitation when determining the failure envelope because in the case of the measured axial and lateral stresses, both quantities are corrupted by error and there is no justification to assume one of them without any error.

Pincus[11] suggests a family of methods to construct the failure envelope piece-wise. Each segment of the envelope is derived from a closed-form solution for two consecutives Mohr circles. Zambrano-Mendoza *et al.*[45] note that while the Pincus method provides great flexibility, it has some drawbacks:

- The resulting envelope is not smoothing (differentiable) at the intersecting point of two segments.

- Construction of the segments, requires pre-processing to create "average circles", this effort is difficult to justify from a statistical point of view.

We represent the rock failure envelope in algebraic form in the Mohr plane by creating the equation of the envelope in such way that the sum of the squares of the distance from the Mohr's circles is minimized. This is achieved by the application of the method of EIVmethod.[29-41] We consider linear, parabolic and hyperbolic models of the failure envelope, but the method can be extended to other models. The applicability of this methodology is illustrated and verified[44] using the well-documented data set published by Pincus, based on the ASTM interlaboratory study.[12-14] The selected data contain triaxial test results conducted in several laboratories at different confining pressure. In this work, we consider triaxial test data for three rocks (Berea sandstone, Barre granite, and Tennessee marble). However, our main interest is to analyze the failure criteria for sedimentary reservoir rock in the near-wellbore region. Our proposed methodology provides a physically sound representation of the failure envelope, because

      a. it does not require segmentation, and hence preserves smoothness

      b. it uses a small number of parameters, and

      c. the optimality criterion has a straightforward physical meaning.

We use the EIV methodology for fitting failure envelopes in the Mohr plane. The derivations of all these equations appear in Appendix A.

3.2.2. Methodology and procedure

The EIV method is applied to obtain the parametric representation of the failure envelope in the Mohr plane. The reconciled stress state satisfies the equation of the envelope in the Mohr plane:

$$f\left(\hat{\sigma}_i, \hat{\tau}_i, \underline{\theta}\right) = 0 \quad\dots\dots\dots\dots\dots\dots\dots\dots\dots\dots\dots\dots\dots\dots\dots\dots\dots\dots\dots(3\text{-}4)$$

where $\underline{\theta}$ is the vector of parameters.

We must modify the EIV method to apply it in the Mohr plane, because a circle, not a point, represents the measurement information. The generalization of the EIV method is straightforward, once the concept of the distance of the Mohr circle from a failure envelope is clarified.

Fig. A-1 is a schematic representation of the EIV approach applied to failure-envelope determination in the Mohr's plane. Reconciliation of the distance from each observed Mohr circle to the envelope requires us to minimize the sum of squares of distances, d_i

$$J = \sum_{i=1}^{n} d_i^2 \quad\dots\dots\dots\dots\dots\dots\dots\dots\dots\dots\dots\dots\dots\dots\dots\dots\dots\dots..(3\text{-}5)$$

The geometric distance in equation (3-5) can be expressed as

$$J = \sum_{i=1}^{n}\left(\sqrt{\left(c_i - \hat{\sigma}_i\right)^2 + \hat{\tau}_i^{\,2}} - r_i\right)^2 \quad\dots\dots\dots\dots\dots\dots\dots\dots\dots\dots\dots\dots(3\text{-}6)$$

We formulate the EIV approach by minimizing J (Eq. 3-6), subject to the constraint of Eq. 3-4.

We derive the parametric equations of the envelopes for the three most frequently used algebraic forms (linear, parabolic, and hyperbolic models) in Appendix

A. Using those equations, we validate the proposed methodology with an appropriate set of triaxial data from different laboratories.

3.2.3. Discussion and results

The ASTM interlaboratory study[12-14] obtained triaxial compressive strength of intact, uniformly oriented, cylindrical specimens. The goal was to obtain all the failure envelopes for the three rocks, using all the available information provided by the various laboratories. Then the resulting failure envelopes to the ones obtained by Pincus was compared.[11]

The selected data consist of triaxial measurements from a series of compressive tests obtained at different laboratories. From these experimental data 83 Mohr's circles for Barre granite and 107 Mohr's circles for both the Berea sandstone and Tennessee marble were constructed. **Table 3-1** contains the optimal parameters for the linear, parabolic, and hyperbolic model for each of the selected rocks. In **Table 3-1** we show the parameters describing the failure envelope located nearest to the n Mohr's circles obtained from data measured in various laboratories under various confining pressures for each kind of rock. The possible use of these parameters is within a computational algorithm, where a stress state needs to be tested for failure. Using the listed parameters, we can minimize the likelihood of making a wrong judgment (i.e. declaring a failure state as safe or a safe state as failure.) **Figs. 3-1** through **3-3** show the linear and parabolic models for the three samples. In the case of the two-parameter parabolic model, we used an additional constraint: the envelope must intersect with the τ axis, which requires $\theta_0 \geq 0$.

The standard deviation is obtained from the sum of the squared distances between the failure envelope and the Mohr's circles (objective function values, **Table 3-2**). For comparison, we calculated the standard deviation for the closed-form model (CFM) envelopes obtained by Pincus.[11] That calculation is not trivial because the CFM

TABLE 3-1- OPTIMAL PARAMETERS DETERMINED FROM THE EIV METHOD IN THE MOHR PLANE

	Linear		Parabolic		Hyperbolic	
	$f(\hat{\sigma},\hat{\tau},\underline{\theta}) = \theta_0 + \theta_1\hat{\sigma} - \hat{\tau}$		$f(\hat{\sigma},\hat{\tau},\underline{\theta}) = \theta_0 + \theta_1\hat{\sigma} - \hat{\tau}^2$		$f(\hat{\sigma},\hat{\tau},\underline{\theta}) = \theta_0 + \theta_1\hat{\sigma}^2 - \hat{\tau}^2$	
	θ_0	θ_1	θ_0	θ_1	θ_0	θ_1
Test rock	MPa	(−)	MPa^2	MPa	MPa^2	(−)
Barre granite[a]	36.9	1.17	17.4	194.6	2728	2.59
Berea sandstone[b]	11.3	0.90	0	67.9	239	1.27
Tennesse marble[b]	22.0	0.87	78.5	89.8	666	1.53

a: 83 Test samples
b: 107 Test samples
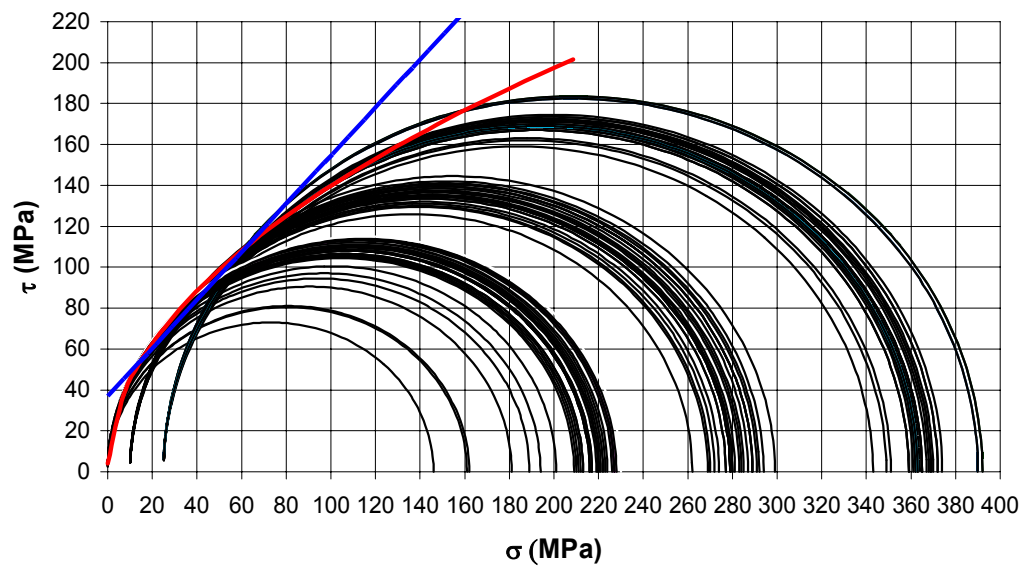
Fig. 3-1-   Parametric representation of the failure envelope in the Mohr plane from EIV for Barre granite (linear and parabolic models).
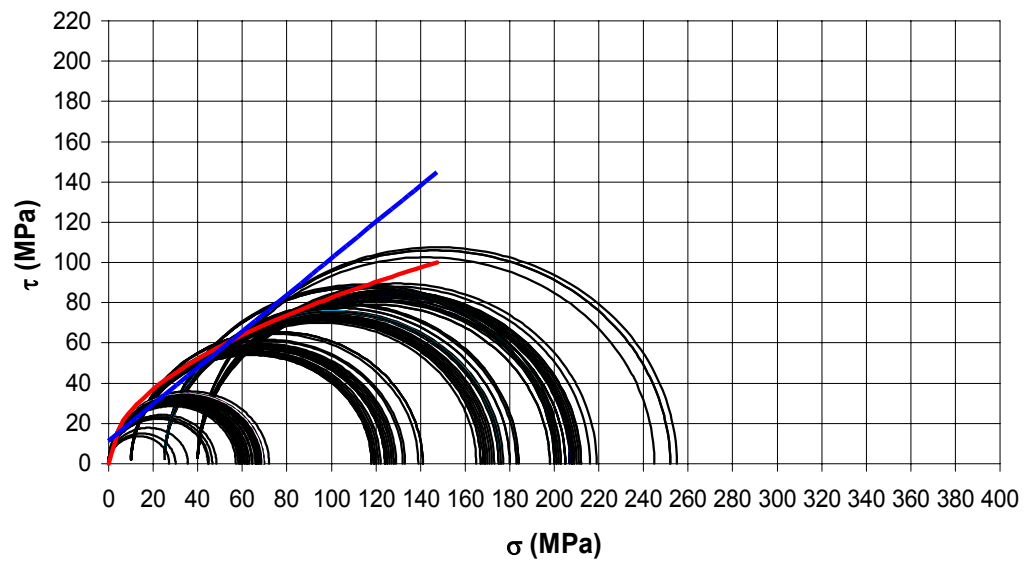
Fig. 3-2- Parametric representation of the failure envelope in the Mohr plane from EIV for Berea sandstone (linear and parabolic models).
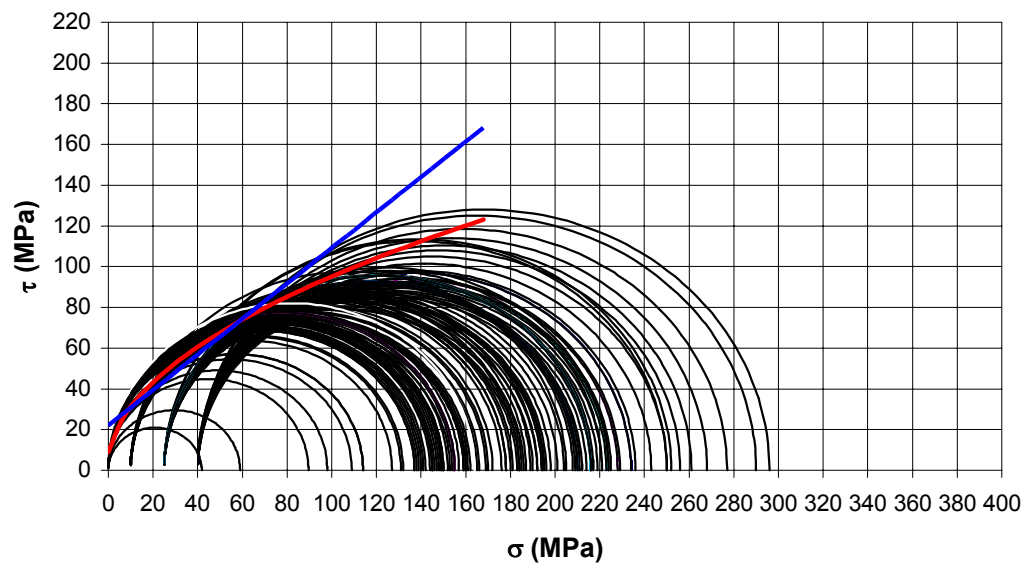
Fig. 3-3- Parametric representation of the failure envelope in the Mohr plane from EIV for Tennessee marble (linear and parabolic models).

TABLE 3-2- STANDARD DEVIATION BETWEEN MOHR'S CIRCLES AND FAILURE ENVELOPE FROM EIV AND SEGMENTED CF ENVELOPE

	Linear		Parabolic		Hyperbolic	
	$f(\hat{\sigma},\hat{\tau},\underline{\theta})=\theta_0+\theta_1\hat{\sigma}-\hat{\tau}$		$f(\hat{\sigma},\hat{\tau},\underline{\theta})=\theta_0+\theta_1\hat{\sigma}-\hat{\tau}^2$		$f(\hat{\sigma},\hat{\tau},\underline{\theta})=\theta_0+\theta_1\hat{\sigma}^2-\hat{\tau}^2$	
	EIV	*CF*	*EIV*	*CF*	*EIV*	*CF*
Test rock	(%)	(%)	(%)	(%)	(%)	(%)
Barre granite[a]	2.2	1.4	1.2	1.8	2.8	3.0
Berea sandstone[b]	7.7	6.7	3.4	7.4	10.1	10.4
Tennesse marble[b]	9.8	7.6	6.3	9.7	11.7	17.2

a: 83 Test samples
b: 107 Test samples

envelope consists of three segments, and the distance of an individual Mohr's circle should be calculated either from the orthogonallity criterion or at the intersection of two segments, while selecting the valid segment. Notice that similar computational difficulties may arise in calculating the tangent of the envelope because the slope changes from one side to the other of each segments end point.

More importantly, the CFM model proposed by Pincus[11], has six model parameters (describing three straight lines for the piece-wise linear model), while the EIV envelope determined here has only either two or three parameters (one straight linefor the linear envelope case). In spite of the smaller number of parameters, the EIV model provides smaller "sum of squared distances" for all models, except the linear model. **Figs. 3-4** and **3-5** illustrate the difference between those two approaches. For an arbitrarily selected Mohr circle, the distance from the EIV envelope is uniquely defined (**Fig. 3-4**); for the segmented CF envelope, we show only two segments with the same Mohr circle in **Fig. 3-5** defining the dotted line as Segment 1, whereas the solid line is Segment 2. If we consider only the formal equation of Segment 1, we obtain the nearest point P_1, but it defines a false distance, because it lies outside the validity domain of the segment. Similarly, P_2 defines a false distance. Therefore, the physically meaningful distance of the Mohr circle from the envelope is defined by the intersection point P_3.

In addition, we suggest a three-parameter hyperbolic model that generates a lower standard deviation. **Fig. 3-6** illustrates a three-parameter model for Berea sandstone including the tensile strength data. The standard deviation obtained in this case is about 4.7%, compared to 8.3% obtained from the two-parameter parabolic EIV model. This program has the option of using weights that depend on whether the envelope crossed the Mohr circle or not. However, that discussion is out of the scope of the present research.

Finally we note that the EIV approach will reproduce an envelope that resembles the traditional failure envelope. For this we consider the average circles given by Pincus[11] for Berea sandstone, which are shown in **Fig. 3-7**. In this figure we observe the

hyperbolic three-parameter envelope perfectly touching the tangential point of each of the four average circles obtained at confining pressures of 0, 10, 25 and 40 MPa. The standard deviation found on this case is about 0.44%.

3.2.4. Conclusions

The EIV procedure can be applied to virtually any failure-envelope model. It provides exactly reproducible envelope parameters from a given set of data. The resulting parameters correspond to a well-defined optimality criterion that makes more statistical and rock-mechanical sense than the traditional least-squares approach because the EIV method accounts for measurement errors in both x and y. The smoothness (differentiability) of the resulting envelope makes it suitable for use in applications requiring a differentiable failure function. We can interpolate within the range of the envelope equation more accurately than with the segmented representations for the nonlinear models.
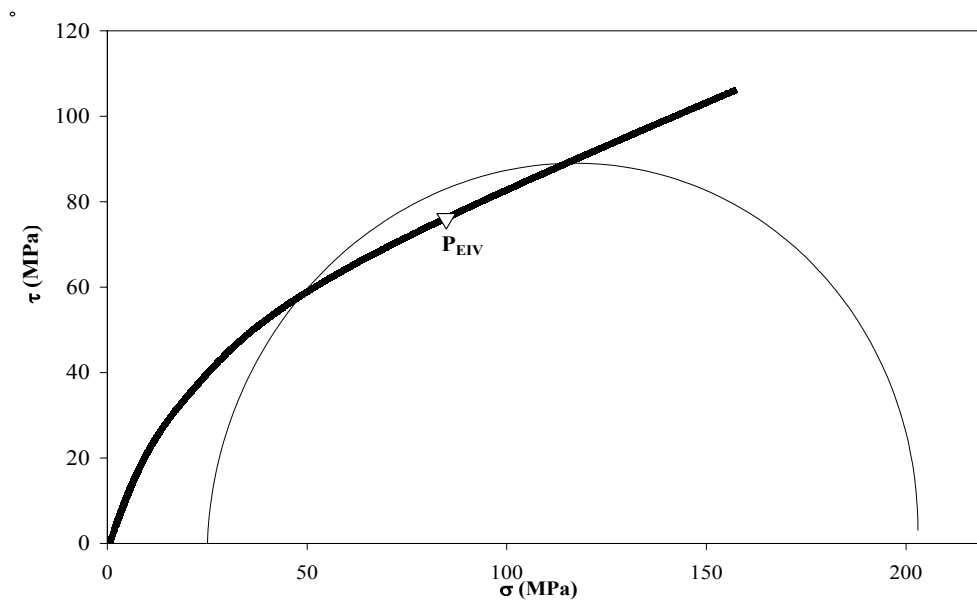
Fig. 3-4- Mohr's circle No 72 for Berea sandstone. Distance from EIV (parabolic) envelope. PEIV: Reconciled point of the circle on the envelope.
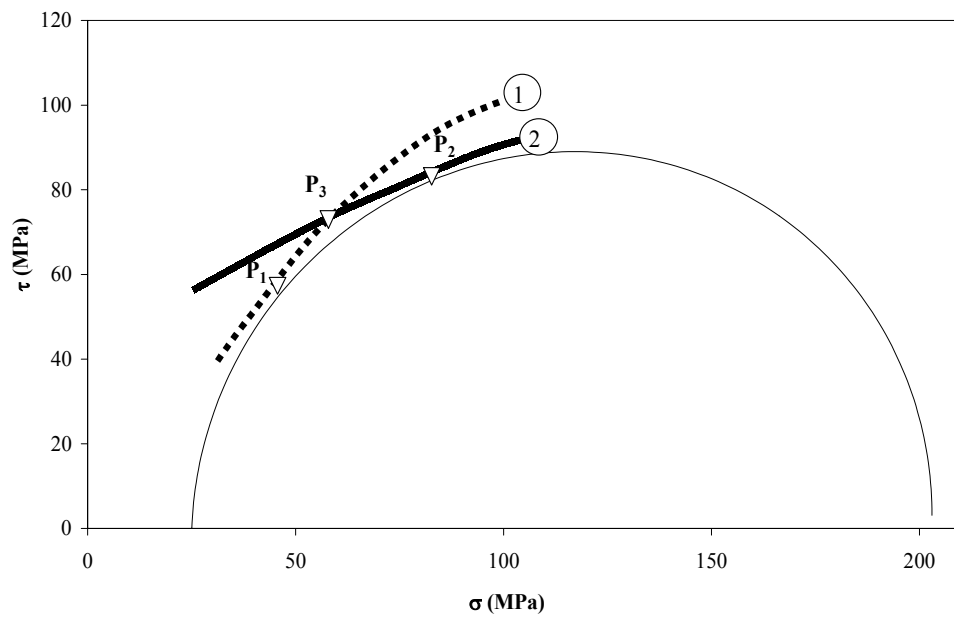
Fig. 3-5- Mohr's circle No 72 for Berea sandstone. Distance from segmented CF (parabolic) envelope.
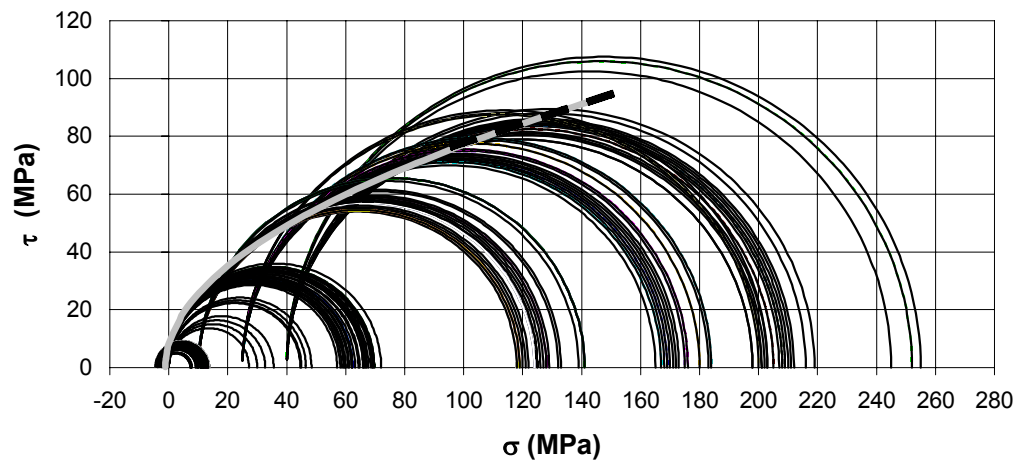
Fig. 3-6- Hyperbolic three-parameter envelope equation from EIV method for Berea sandstone (tensile strength data from a Brazilian test included). The dashed line is an extrapolation of the failure envelope.
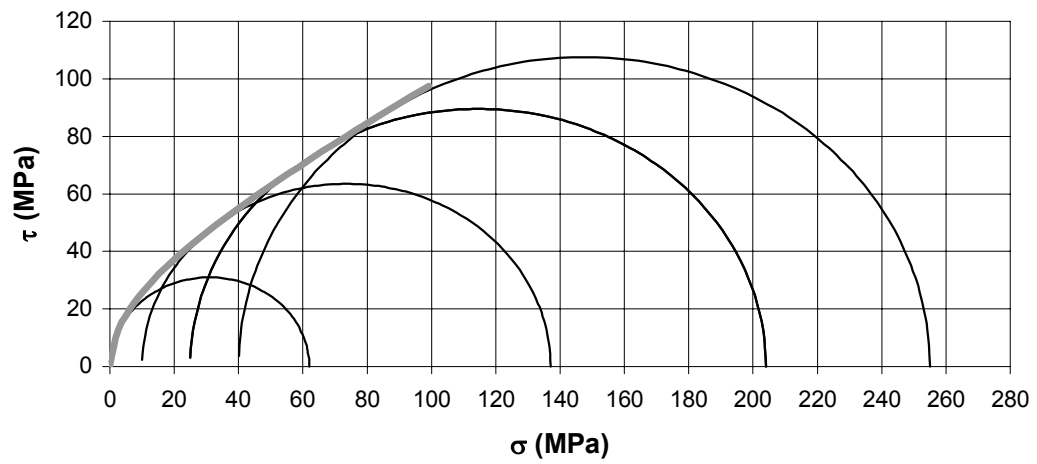
Fig. 3-7- Hyperbolic three-parameter envelope equation from EIV method for Berea sandstone using average circles.

3.3. Fitting failure envelope in the principal stress plane.

3.3.1. Introduction

The physical limitation of the experimental setup mostly forces us to represent the failure criteria in the stress-state plane, neglecting the intermediate principal-stress influence. If we assume that the effect of the intermediate principal stress does not influence the rock strength (which is not always true), we can express a failure criterion in terms of the major (σ_1) and minor (σ_3) principal stresses and represent the criterion by Eq. 3-1.

Several empirical failure criteria have arisen over the past five decades in the attempt to simulate the triaxial behavior of in-situ (intact) rock specimens. The majority of those equations were proposed for a few particular rock types having in each case a limited number of data.[20] In 1980, Hoek and Brown[21] developed a new failure equation and fitted it comprehensively to different rock types. Similarly to most empirical failure criteria, it was formulated in terms of σ_1 and σ_3 and independent of σ_2. Some of the empirical failure envelope equations were assumed only in the compression and did not necessarily exist in the tensile quadrant. This implies a limitation because a failure criterion should exist both in the tensile and compressive region to be comprehensive enough.[22] Sheorey [23] provides a list of the most relevant empirical failure equations.

The least-squares method has been widely adopted to fit the failure envelope directly from the experimental data. Mostyn and Douglas[22] presented different results fitting the different forms of the Hoek and Brown[21] criterion.

We present the parametric representation of the rock-strength failure envelope in the principal-stress plane and the transformation of the resulting envelope into the Mohr plane. In the suggested method, we first fit an envelope to the measured axial and lateral stresses at failure using the statistical method of error-in-variables that does not make an artificial distinction between independent and dependent variables. We used linear and

parabolic algebraic forms to represent the envelope equations. Then we transform the envelope into the Mohr plane. To accomplish the transformation from the principal stress plane to the Mohr plane, we use Balmer's solution strengthened with computer algebra. We illustrate and verify the EIV method application using a well-documented set of data collected from the previous work of Pincus[12-14] and Sheorey.[23] We use triaxial tests data for different sandstones, which include tensile strength measurements. To test the improvement provided by this method, we compare the calculated objective function (likelihood of erroneous decision) with the parametric representation obtained using various least-squares methods.[12-14] We found that our proposed methodology, which is based on the statistical method of error-in-variables reinforced with a transformation process, has two advantages:

- It simplifies the process of creating a failure envelope for practical applications.
- It minimizes the likelihood of erroneous judgment during applications (i.e. indicating failure in a stable state or vice versa.

The derivation of all the equations to fit the failure envelope in the principal stress using EIV and the process of transform the resulting parametric solution appear in Appendix A.

3.3.2. Methodology and procedure

In the principal stress plane, the model can be written in its implicit form as:

$$g(\hat{\sigma}_3, \hat{\sigma}_1, \underline{\theta'}) = 0 \dots\dots\dots\dots\dots\dots\dots\dots\dots\dots\dots\dots\dots\dots\dots(3\text{-}7)$$

Our goal is to find the optimum parameters, at which the sum of necessary corrections squared,

$$J = \sum_{i=1}^{n} d^2_{p_i} ,\ldots\ldots\ldots\ldots\ldots\ldots\ldots\ldots\ldots\ldots\ldots\ldots\ldots\ldots\ldots\ldots\ldots\ldots\ldots\ldots\ldots.(3\text{-}8)$$

is minimum, where for each pair of measurements, the squared distance is given by

$$d^2_{p_i} = \left(\hat{\sigma}_{3i} - \sigma_{3i}\right)^2 + \left(\hat{\sigma}_{1i} - \sigma_{1i}\right)^2 \ldots\ldots\ldots\ldots\ldots\ldots\ldots\ldots\ldots\ldots\ldots\ldots\ldots..(3\text{-}9)$$

In Appendix A, Fig. A-3 is the schematic representation of the correction or reconciliation that corresponds to the true distance of the point from the algebraic curve using the EIV method (d_{pi}).

Thus, minimizing Eq. 3-8 subject to the constraint of Eq. 3-7 constitutes the EIV formulation. The simple form of the objective function Eq. 3-7 allows us to use the EIV algorithm presented in Appendix A and the derived equations for the linear and parabolic model to derive the parametric equations of the envelope. Using those equations, we can validate the proposed methodology with an appropriate set of triaxial data. In the following we show some outcomes after applying the EIV-based method to a well-documented data set.[12-14,23]

Once we have derived the parametric representation of the failure envelope using the EIV method through one of the algebraic forms described above, we can generalize Balmer's solution on the Mohr' failure criterion to map out resulting envelope into the Mohr plane.

3.3.2.1. Transformation of the parametric representation of the failure envelope from the principal stress plane into the Mohr plane.

Using the EIV parametric representation of the failure envelope in the principal stress plane [Eq. (3-7)] we can transform the algebraic solution to a parametric representation into the Mohr plane. To accomplish this task, we used Balmer's solution of the Mohr failure criterion, which is based on the principal-stress components. Introducing the

reconciled value of $(\hat{\sigma}_3, \hat{\sigma}_1)$ obtained from the EIV method in the principal stress plane, in Balmer's equations we can expressed the normal and shear stress as:

$$\hat{\sigma} = \hat{\sigma}_3 + \frac{\hat{\sigma}_1 - \hat{\sigma}_3}{\dfrac{d\hat{\sigma}_1}{d\hat{\sigma}_3} + 1} ,\dotfill (3\text{-}10)$$

and

$$\hat{\tau} = \frac{\hat{\sigma}_1 - \hat{\sigma}_3}{\dfrac{d\hat{\sigma}_1}{d\hat{\sigma}_3} + 1}\sqrt{\frac{d\hat{\sigma}_1}{d\hat{\sigma}_3}} ,\dotfill (3\text{-}11)$$

where

$$\frac{d\hat{\sigma}_1}{d\hat{\sigma}_3} = \frac{dg(\hat{\sigma}_3, \hat{\sigma}_1, \underline{\theta'})}{d\hat{\sigma}_3} \dotfill (3\text{-}12)$$

Solving simultaneously Eqs. 3-7, 3-10 and 3-11, considering Eq. 3-12 a parametric solution in the (σ, τ) stress plane we obtain for the failure envelope

$$f(\hat{\sigma}, \hat{\tau}, \underline{\theta'}) = 0 \dotfill (3\text{-}13)$$

We must emphasize that the implicit form resulting from the transformation process Eq. 3-13 is a function of the parameters obtained in the principal stress plane. It is important to note that a closed-form solution may or may not be achieved analytically. In this work we consider cases when a closed-form solution can be found using Computer Algebra software.

To illustrate the transformation of the failure envelope from the principal-stress plane to the Mohr plane, we present how the parametric representation of the linear and parabolic models obtained in the principal-stress plane are mapped into the Mohr plane. The derivations of the transformation process from the principal stress plane to the Mohr plane based on Balmer's solution of the Mohr failure criterion and the concept of EIV appear in Appendix A.

3.3.2.1.1. Transformation of selected model

Let us assume that we already have obtained the EIV parametric representation of the failure envelope in the principal-stress plane. That is, we have determined the optimum parameters of the linear and parabolic model. For the linear model,

$$g(\hat{\sigma}_{3i}, \hat{\sigma}_{1i}, \underline{\theta'}) = \theta'_0 + \theta'_1 \hat{\sigma}_{3i} - \hat{\sigma}_{1i} = 0 \quad \text{...}(3\text{-}14)$$

Then Eq. 3-12 represents

$$\frac{d\hat{\sigma}_1}{d\hat{\sigma}_3} = \frac{dg(\hat{\sigma}_{3i}, \hat{\sigma}_{1i}, \theta')}{d\hat{\sigma}_3} = \theta'_1 \quad \text{...} \quad (3\text{-}15)$$

Then the resulting parametric solution in the (σ, τ) stress plane is expressed as

$$f(\hat{\sigma}_i, \hat{\tau}_i, \theta') = \frac{\sqrt{\hat{\sigma}_i^2 - 2\hat{\sigma}_i\theta'_0 + \theta'^2_0 - 2\hat{\sigma}_i^2\theta'_1 + 2\hat{\sigma}_i\theta'_0\theta'_1 + \hat{\sigma}_i^2\theta'^2_1}}{\sqrt{\theta'_1}} - \hat{\tau}_i \quad (3\text{-}16)$$

The parabolic model can also be transformed into a parametric representation in the Mohr plane.

$$g(\hat{\sigma}_{3i},\hat{\sigma}_{1i},\underline{\theta'})= \theta'_0 + \theta'_1 \hat{\sigma}_{3i} - \hat{\sigma}_{1i}^2 = 0 \dots\dots\dots\dots\dots\dots\dots\dots\dots\dots\dots\dots(3\text{-}17)$$

To transform into the Mohr plane, we derive Eq. 3-17 to Eq. 3-13 as

$$\frac{d\hat{\sigma}_1}{d\hat{\sigma}_3} = \frac{dg(\hat{\sigma}_{3i},\hat{\sigma}_{1i},\theta')}{d\hat{\sigma}_3} = \frac{\theta'_1}{2\sqrt{\theta'_0 + \theta'_1\hat{\sigma}_{3i}}} \dots\dots\dots\dots\dots\dots\dots\dots\dots\dots\dots(3\text{-}18)$$

This process is shown in detail in Appendix A. Then the resulting parametric solution in the (σ,τ) stress plane is expressed as

$$f(\hat{\sigma}_i,\hat{\tau}_i,\theta') = -\frac{2\hat{\sigma}_i^2}{3} + \frac{2\hat{\sigma}_i}{27\theta'_1} - \frac{2\hat{\sigma}_i\theta'_0}{3\theta'_1} + \frac{2(\sigma_i^2 + 3\theta'_0 + 3\sigma_i\theta'_1)^{3/2}}{27\theta'_1} - \tau_i^2 \dots\dots(3\text{-}19)$$

Since the slope $\dfrac{d\hat{\sigma}_1}{d\hat{\sigma}_3}$ given by equation (3-19) must exist, the square root term must be greater than or equal to zero. In addition, because the slope depends on σ_3 it should increase when the values of these variables increase; thus, the slope must be positive. This implies that an envelope generated this way can describe the failure criteria for the brittle region but not the brittle/ductile region of the tested rock.

We assumed that the quantity under the square root is always positive; this implication is automatically satisfied, in the brittle region.

3.3.3. Discussion and results

To illustrate and verify the applicability of the EIV method to fit the failure envelope in the principal-stress plane, we processed the results of a previous ASTM interlaboratory study[12-14] assuming only linear and parabolic envelope models (although our technique can be extended to other models). In this study, the triaxial compressive strength of intact, uniformly oriented cylindrical specimens of Berea sandstone, were obtained. Our

goal was to obtain the failure envelopes for this rock in the principal-stress plane, using all the available information provided by the various laboratories. Then we compared the failure envelopes to the ones obtained using least squares. For Berea sandstone, 107 and 147 (including tensile strength) pairs of axial and lateral stresses measurements[1-3] were available. **Table 3-3** and **Table 3-4** contain the optimal parameters for Berea sandstone obtained from EIV and LS methods respectively. **Table 3-3** shows the parameters described by the failure envelope located nearest to the 107 and 147 pairs of axial and lateral-stress measurements obtained from data measured in various laboratories under various confining pressures. The possible use of these parameters is within a computational algorithm where a stress state needs to be tested for failure. The likelihood of making a wrong judgment (i.e. declaring a failure state as safe or a safe state as failure) can be minimized by these parameters.

The standard deviation is obtained from the sum of the squared distances between the failure envelope and each pair of measurements (objective function values); the standard deviations are shown in **Table 3-5**. For comparison, we calculated the standard deviation using least squares. The EIV model provides smaller "sum of squared distances" for the rock and both of the selected models. **Fig. 3-8** show the parametric representation of the failure envelope obtained from EIV and LS method for the parabolic models. To reinforce the goodness of the EIV method to obtain the parametric representation of the failure envelope in the principal stress plane, we compared it with the well-establishes method of Hoek & Brown[21] and Balmer[10] using a set of sandstone data presented by Sheorey.[23] The selected data contained at least 5 pairs of measurements

TABLE 3-3-OPTIMAL PARAMETERS DETERMINED FROM THE EIV METHOD IN THE PRINCIPAL STRESS PLANE

Test rock	Linear		Parabolic	
	$g(\hat{\sigma}_3,\hat{\sigma}_1,\underline{\theta'})=\theta'_0+\theta'_1\hat{\sigma}_3-\hat{\sigma}_1$		$g(\hat{\sigma}_3,\hat{\sigma}_1,\underline{\theta'})=\theta'_0+\theta'_1\hat{\sigma}_3-\hat{\sigma}_1^2$	
	θ_0	θ_1	θ_0	θ_1
	MPa	(−)	MPa^2	MPa
Berea sandstone[a]	64.71	4.22	3291.76	1133.43
Berea sandstone[b]	45.43	5.01	3751.69	1116.84

07 Test samples

47 Test samples (Include tensile strength)

TABLE 3-4- PARAMETERS DETERMINED FROM LEAST-SQUARES METHOD IN THE PRINCIPAL STRESS PLANE

	Linear		Parabolic	
	$g(\hat{\sigma}_3, \hat{\sigma}_1, \underline{\theta'}) = \theta'_0 + \theta'_1\hat{\sigma}_3 - \hat{\sigma}_1$		$g(\hat{\sigma}_3, \hat{\sigma}_1, \underline{\theta'}) = \theta'_0 + \theta'_1\hat{\sigma}_3 - \hat{\sigma}_1^2$	
	θ_0	θ_1	θ_0	θ_1
Test rock	MPa	(−)	MPa^2	MPa
Berea sandstone[a]	70.22	3.89	3594.18	1105.80
Berea sandstone[b]	50.08	4.60	3751.69	1135.64

a: 107 Test samples

b: 147 Test samples (Include tensile strength)

TABLE 3-5- STANDARD DEVIATION BETWEEN MEASUREMENTS AND FAILURE ENVELOPE FROM EIV AND LEAST-SQUARES ENVELOPE

	Linear		Parabolic	
	$g(\hat{\sigma}_3, \hat{\sigma}_1, \underline{\theta'}) = \theta_0' + \theta_1'\hat{\sigma}_3 - \hat{\sigma}_1$		$g(\hat{\sigma}_3, \hat{\sigma}_1, \underline{\theta'}) = \theta_0' + \theta_1'\hat{\sigma}_3 - \hat{\sigma}_1^2$	
	EIV	LS	EIV	LS
Test rock	(%)	(%)	(%)	(%)
Berea sandstone[a]	4.31	18.14	3.76	12.93
Berea sandstone[b]	4.64	22.75	3.23	12.68

a: 107 Test samples

b: 147 Test samples (Include tensile strength)
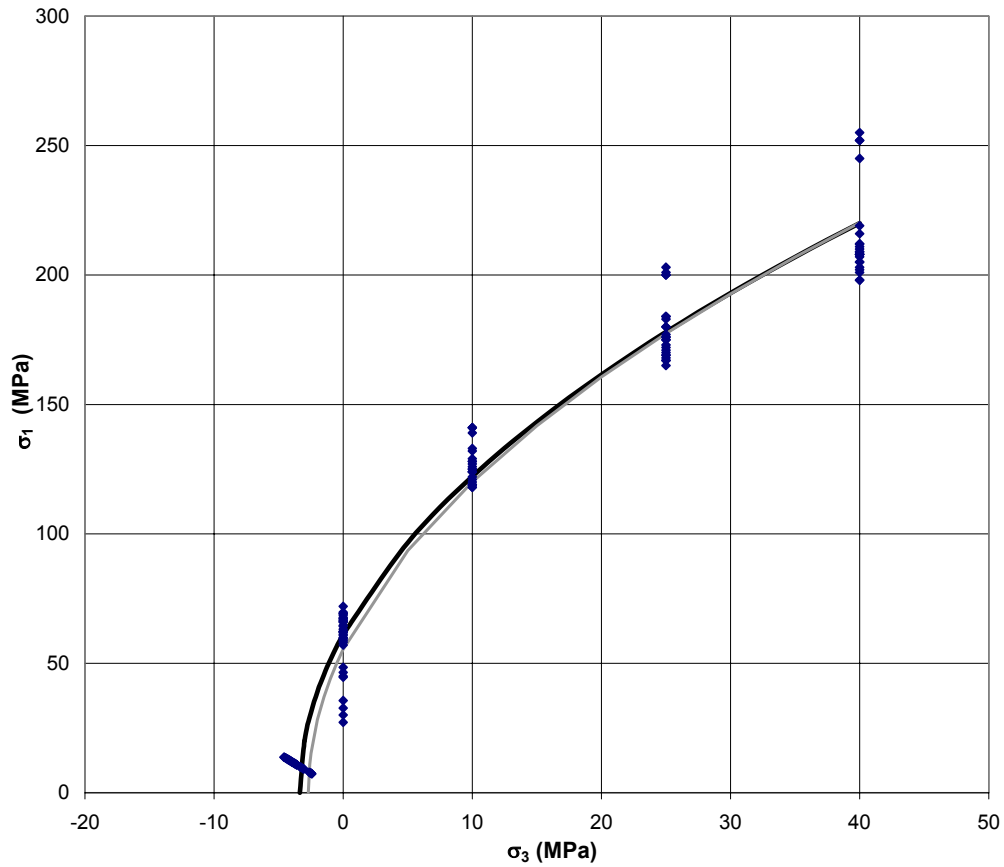
Fig. 3-8- Parametric representation of the failure envelope in the principal stress plane using EIV and least-square method for Berea sandstone parabolic model. Including indirect tensile strength data. Black solid curve represent the EIV method while gray solid curve represent the least-square method.

TABLE 3-6- COMPARATIVE ANALYSIS BETWEEN EIV, BALMER AND HOEK & BROWN METHODS.

Set no	EIV			Balmer				Hoek & Brown			
	σ_c	σ_t	r^2	σ_c	σ_t	b	r^2	σ_c	σ_t	m	r^2
32	123.6	10.22	0.978	125.9	8.85	0.452	0.978	129.9	18.15	7.017	0.906
33	113.4	9.59	0.997	113.3	10.53	0.523	0.991	112.9	14.68	7.561	0.978
49	108.5	5.44	0.999	104.3	4.85	0.494	0.999	109.0	8.11	13.367	0.994
57	12.9	0.21	0.983	21.7	0.71	0.521	0.994	21.7	0.88	24.537	0.999
58	138.7	8.25	0.992	127.1	4.83	0.444	0.992	152.4	16.54	9.110	0.927
68	42.4	2.56	0.981	41.2	2.96	0.577	0.983	41.5	2.92	14.123	0.938
134	93.5	3.40	0.990	106.0	7.19	0.591	0.997	110.7	7.26	15.174	0.992
135	90.7	4.56	0.990	85.0	4.07	0.504	0.990	98.8	8.09	12.125	0.958
136	84.5	4.34	0.955	91.6	4.39	0.462	0.956	103.6	10.63	9.643	0.864
137	101.2	7.92	0.989	91.1	5.71	0.483	0.990	104.2	13.39	7.652	0.950
162	27.4	0.78	0.994	37.8	2.09	0.550	0.998	44.2	3.39	12.972	0.999
163	54.2	2.84	0.997	54.2	2.62	0.486	0.996	61.0	5.75	10.510	0.982
164	44.5	1.66	0.999	44.3	2.28	0.556	0.999	48.2	2.87	16.759	1.000
165	98.5	5.16	0.998	94.0	4.74	0.505	0.998	99.5	7.39	13.379	0.990
166	165.8	13.20	0.927	174.9	10.00	0.377	0.998	162.1	16.47	9.741	0.959
167	100.3	4.15	0.999	96.3	4.02	0.510	0.999	102.1	5.82	17.498	0.997
168	108.1	4.42	0.996	91.5	2.99	0.496	0.999	110.3	6.33	17.382	0.994
177	30.1	2.87	0.989	27.1	1.80	0.458	0.994	28.9	3.93	7.261	0.961
183	47.5	0.91	0.993	64.8	3.01	0.603	0.999	54.8	1.56	35.107	0.998
191	67.1	4.52	0.998	66.2	4.72	0.527	0.998	64.8	5.02	12.824	0.995

σ_c: uniaxial compressive strength

σ_t: tensile strength

b: Balmer's parameter

m: Hoek & Brown's parameter

r^2: index of determination

and reported at least one tensile-strength measurement. **Table 3-6** shows the results. We note that even if the number of parameters (two) for the parabolic model using the EIV method is lower than that for the Hoek & Brown and Balmer methods, the resulting r^2 when using EIV is in most cases lower than the one obtained by either one of the other methods. The index of determination r^2 is defined by

$$r^2 = 1 - \frac{\sum [\hat{\sigma}_{1i} - g(\hat{\sigma}_{3i})]^2}{\sum \hat{\sigma}_{1i}^2 - \left(\sum \hat{\sigma}_{1i}\right)^2 / n} \quad\text{..(3-20)}$$

for a failure criterion $\sigma_1 = g(\sigma_3)$, with $(\sigma_{3i}, \sigma_{1i})$ being the *i*-th data pair and *n* the number of data pairs.[23]

To verify the accuracy of transforming the resulting parametric representation of the failure envelope in the principal stress plane to the Mohr plane, we used the calculated values of θ'_0 and θ'_1, which are the parameters of the parabolic envelope given in **Table 3-3** for Berea sandstone[12-14] in the compressive region. For this case, if we use the parabolic model to represent the failure envelope in the Mohr plane,[45] we obtain a lower standard deviation, but the resulting envelope could cross out the plane close to the origin of coordinates, distorting the estimation of the uniaxial compressive strength σ_c and tensile strength σ_t. From the transformation, the resulting equation that represents the failure envelope in the Mohr plane represents a lower sum of squared distance than the one obtained when fitting the envelope directly in the Mohr plane using the EIV method for the parabolic model. **Fig. 3-9** shows the failure envelope obtained from transformation of the parabolic model in the principal stress plane into the Mohr plane, whereas **Fig. 3-10** shows the failure envelope fitted directly in the Mohr plane using the parabolic model. Comparing **Figs. 3-9** and **3-10**, we notice that the standard deviation given by

$$S.Dev = \sqrt{\frac{J}{n-2}} \quad\text{...(3-21)}$$

is ±3.05 MPa when fitting the failure envelope directly in the Mohr plane using the parabolic model and ± 2.91 MPa when using the transformation procedure.

3.3.4. Conclusions

The EIV method can improve the parametric representation of the failure envelope in the principal stress plane. The resulting EIV nonlinear envelope equation, which can be transformed into the Mohr plane, provided a more appropriate and accurate approximation than the one obtained when fitting the failure envelope directly in the Mohr plane.

3.4. Fitting failure envelope including poroelastic effect

3.4.1. Introduction

A failure criterion can be represented as a relation between the principal effective stresses components. In the presence of pore fluids, the mechanical properties of porous rocks depend on both pore-fluid pressure and confining pressure according to the Terzagui effective pressures law,[4] which can be used for many rock types and physical properties in its more general form as $p_e = p_c - \alpha p_p$, where α is a constant (usually referred to as

Biot's constant) that takes on different values for different materials but is always less than or equal to one.[7]

The parametric equations of the failure envelope can be obtained by introducing the concept of poroelasticity of Biot,[27] representing the state of stress by the effective mean stress (σ'_m) and the equivalent stress (σ_{eq}). The measurements (as well as any variable derived from them) are considered corrupted by experimental error.
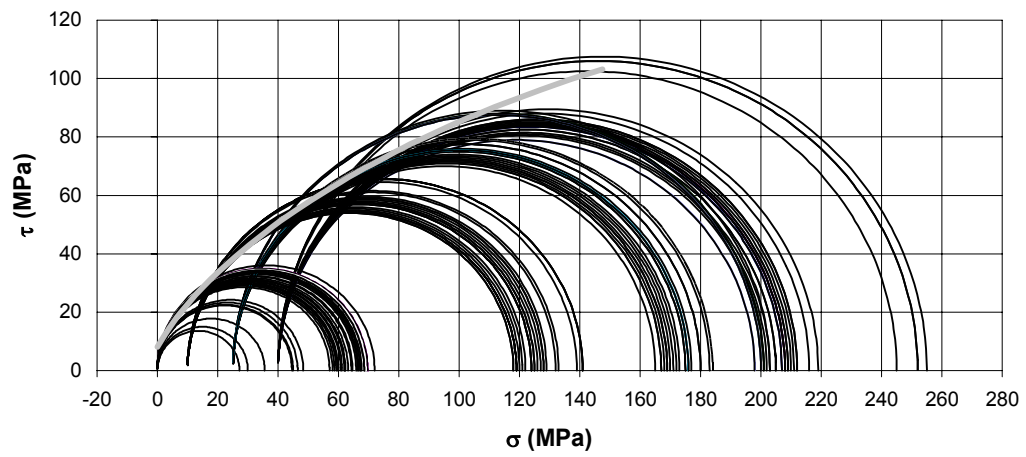
Fig. 3-9- Failure envelope fitting through tansformation from the principal stress plane to the Mohr plane using EIV method (parabolic model).
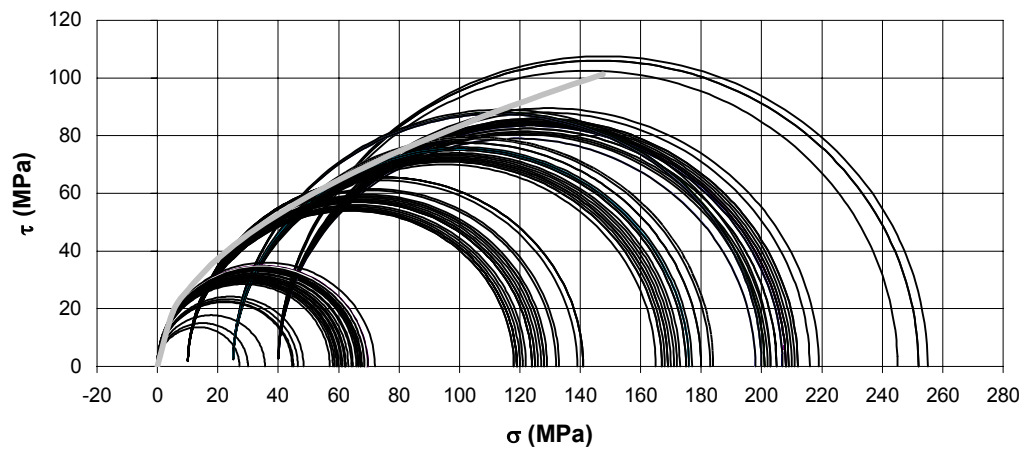
Fig.3-10- Failure envelope fitting directly to the Mohr plane using EIV method (parabolic model)

Nonlinear algebraic forms are considered to fit the failure envelope. To illustrate the application of this methodology, we use a pore-pressure study on Berea sandstone by Aldrich.[42] This part of our research is an extension of a previous work[45], which validated the improvement, achieved using the EIV method to fit the failure envelope in the Mohr plane.[45]. In this part of the research, we provide the application of the EIV- based methodology to fit the envelope in the principal-effective stress plane and considering the brittle/ductile region of the envelope. Later in we formulated the parametric representation of the envelope describing brittle/ductile transition and pore collapse (cap model). Our proposed methodology provides an accurate way of obtaining the parametric representation of the failure envelope describing the deformation mechanism and indicates whether a given stress state will lead to failure or not.

If we assume the effect of the principal intermediate stress has no influence upon the rock strength (triaxial test), this failure criterion can be expressed in terms of the effective mean stress (σ'_m) and the equivalent stress (σ_{eq}), which can be represented by

$$h(\sigma'_m, \sigma_{eq}) = 0 \,\ldots\ldots\ldots\ldots\ldots\ldots\ldots\ldots\ldots\ldots\ldots\ldots\ldots\ldots\ldots\ldots\ldots\ldots\ldots\ldots\ldots\ldots \quad (3\text{-}22)$$

To fit the failure envelope in the principal stress plane we used experimental data from a pore pressure study on Berea sandstone.[42] We use our previously derived formulations developed to represent the failure envelope in the principal stress plane to construct an appropriate model to describe the deformation mechanism of those sedimentary reservoir rocks involving brittle/transition/ductile behavior in the deformation mechanism when we consider pore pressure effects.

3.4.2. Methodology and procedure

Biot,[27] showed that the state of stress can be represented by the effective mean stress (σ_m') and the equivalent stress (σ_{eq}). For the usual triaxial compression test, σ_m' and σ_{eq} are

$$\sigma_m' = (\sigma_1 + 2\sigma_3)/3 - \alpha p_p \quad\quad\quad\quad\quad\quad\quad\quad\quad\quad (3\text{-}23)$$

and

$$\sigma_{eq} = \sqrt{3J_2} = \sigma_1 - \sigma_3 \quad\quad\quad\quad\quad\quad\quad\quad\quad\quad (3\text{-}24)$$

where J_2 represents the second invariant of the stress-deviator tensor and p_p the reservoir pore pressure, and $\alpha = 1 - \dfrac{c_{ma}}{c_b}$ (c_{ma} is the matrix compressibility; c_b is the bulk compressibility).

For highly porous weak sandstones: $c_{ma} << c_b$, so α approaches 1.

Using the EIV approach, we generate an algebraic solution for the material that will satisfy the equation of the envelope given in implicit form as

$$h(\hat{\sigma}_m', \hat{\sigma}_{eq}, \underline{\theta''}) = 0 \quad\quad\quad\quad\quad\quad\quad\quad\quad\quad (3\text{-}25)$$

with a procedure similar to the EIV approach used in (σ_3, σ_1) stress plane.

Our goal is to find the optimum parameters, at which the sum of necessary corrections squared,

$$J = \sum d_{pi}^2 \quad\quad\quad\quad\quad\quad\quad\quad\quad\quad (3\text{-}26)$$

is minimum, expressing the squared distance in terms of the mean effective stress and the equivalent stress as follow:

$$d_{p_i}^2 = \left(\hat{\sigma}'_{mi} - \sigma'_{mi}\right)^2 + \left(\hat{\sigma}_{eqi} - \sigma_{eqi}\right)^2 \quad \text{...} \quad (3\text{-}27)$$

Minimizing Eq. 3-26 subject to the constraint of Eq. 3-25 constitutes the error-in-variable formulation.

The EIV algorithm use to derive the parametric equations of the envelope and the derived equations for the nonlinear algebraic form of the envelope are presented in Appendix A. Using those equations, we can validate the proposed methodology with an appropriate set of triaxial data from different laboratories. In the following we show some outcome after applying EIV based method to a pore pressure study on Berea sandstone.[42]

3.4.3. Discussion and results

To illustrate the applicability of the EIV method to fit the failure envelope in the principal effective stress plane, we used a previous set of experiments involving pore pressure measurement.[42] Three nonlinear parametric functions were considered to fit the envelope. Our goal was to obtain the failure envelopes for Berea sandstone considering pore pressure. **Table 3-7** contains the optimal parameters for the three models.

The standard deviation is obtained from the sum of the squared distances between the failure envelope and each pair of measurements (objective function values); the standard deviations are shown in **Table 3-8**; the standard deviation is given by

$$S.D = \sqrt{\frac{J}{n-2}} \quad \text{...} \quad (3\text{-}28)$$

or

$$S.D = \sqrt{\frac{J}{n-3}} \quad \ldots\ldots\ldots\ldots\ldots\ldots\ldots\ldots\ldots\ldots\ldots\ldots\ldots\ldots\ldots\ldots\ldots\ldots\ldots\ldots(3\text{-}29)$$

according to the degree of freedom of each select functions. **Fig. 3-11** show the parametric representation of the envelope for the given experimental data for those selected models the solid black line represents the parabolic model while the dotted black and solid gray represent the three-parameters parabolic and hyperbolic model respectively. From **Table 3-8** we can infer that the best parametric representation of the

failure envelope were obtained from the three-parameters models, resulting the lowest standard deviation for the three-parameters parabolic model.

3.4.4. Conclusions

The EIV method can provide a simple way to obtain the parametric representation of the envelope in the principal stress plane if we consider the pore-pressure influence describing a more appropriate form of the deformation mechanism for the tested rock.

**TABLE 3-7- OPTIMAL PARAMETERS DETERMINED FROM EIV METHOD
INCLUDING PORE PRESSURE EFFECT**

	Parabolic		Parabolic			Hyperbolic		
	$f(\hat{\sigma}'_m, \hat{\sigma}_{eq}, \underline{\theta''}) = \theta''_0 + \theta''_1 \hat{\sigma}'_m - \hat{\sigma}_{eq}^2$		$f(\hat{\sigma}'_m, \hat{\sigma}_{eq}, \underline{\theta''}) = \theta''_0 + \theta''_1 \hat{\sigma}'_m - \theta''_2 \hat{\sigma}_{eq} - \hat{\sigma}_{eq}^2$			$f(\hat{\sigma}'_m, \hat{\sigma}_{eq}, \underline{\theta''}) = \theta''_0 + \theta''_1 \hat{\sigma}'_m + \theta''_2 \hat{\sigma}'^2_m - \hat{\sigma}_{eq}^2$		
	θ''_0	θ''_1	θ''_0	θ''_1	θ''_2	θ''_0	θ''_1	θ''_2
Test rock	MPa^2	MPa	MPa^2	MPa	MPa	MPa^2	MPa	(-)
Berea sandstone	3.1E-6	398.7	1.2E-7	1254.2	450.5	5.5E-11	127.1	2.4

27 Test samples

TABLE 3-8- STANDARD DEVIATION BETWEEN MEASUREMENTS AND FAILURE ENVELOPE FROM EIV IN THE EFFECTIVE-STRESS PLANE

	Parabolic	Parabolic	Hyperbolic
	$f(\hat{\sigma}'_m,\hat{\sigma}_{eq},\underline{\theta}'')=\theta''_0+\theta''_1\hat{\sigma}'_m-\hat{\sigma}_{eq}{}^2$	$f(\hat{\sigma}'_m,\hat{\sigma}_{eq},\underline{\theta}'')=\theta''_0+\theta''_1\hat{\sigma}'_m-\theta''_2\hat{\sigma}_{eq}-\hat{\sigma}_e$	$f(\hat{\sigma}'_m,\hat{\sigma}_{eq},\underline{\theta}'')=\theta''_0+\theta''_1\hat{\sigma}'{}_m+\theta''_2\hat{\sigma}'^2_m-\hat{\sigma}_{eq}{}^2$
	EIV	*EIV*	*EIV*
Test rock	Percent	Percent	Percent
Berea sandstone	11.0	4.6	5.4

27 Test samples
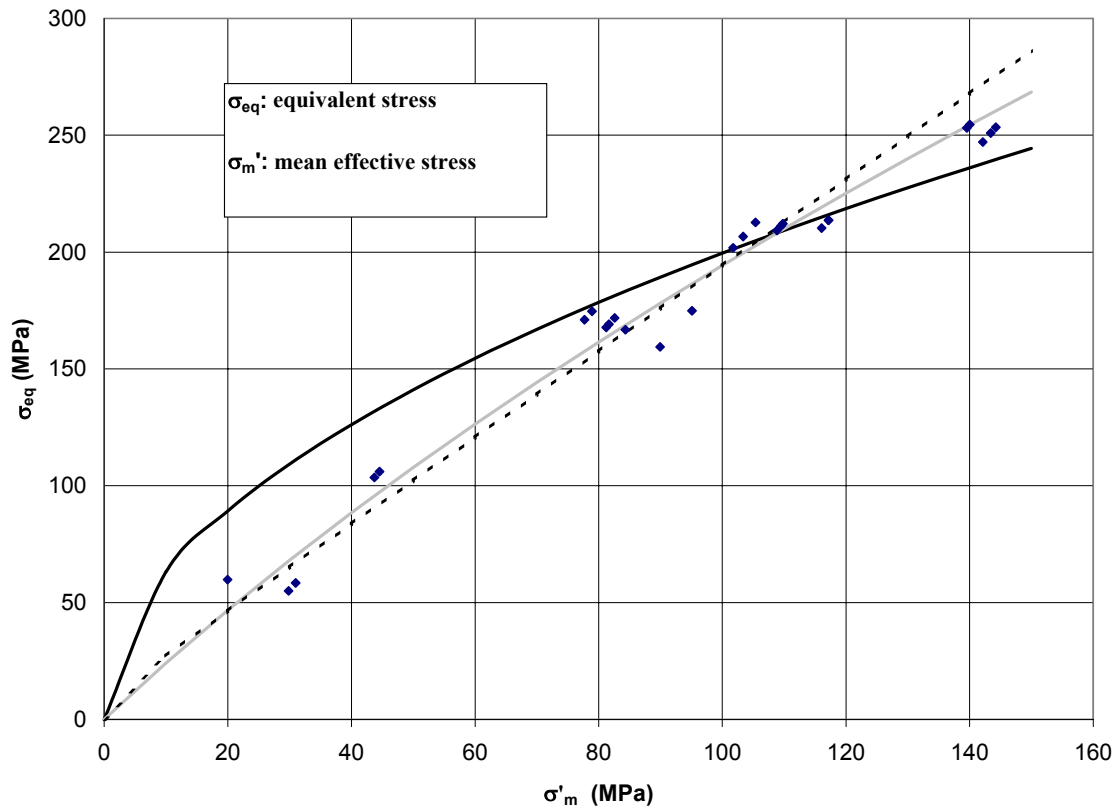
Fig. 3-11- Parametric representation of the failure envelope in the principal stress plane considering pore pressure effect using EIV method for Berea sandstone (parabolic two and three, and hyperbolic three-parameters, models). Black solid curve represents the two-parameter parabolic model, the black dashed curve represents the thrre-parameter parabolic model while the gray solid curve represents the three-parameter hyperbolic model.

3.5. Applying the method to special models suitable for describing brittle/ductile transition in the yield envelope

3.5.1. Introduction

A parametric representation describing the deformation mechanism of the porous rock can be achieved by a method of curve fitting. The behavior of porous sandstones undergoing pore collapse and compaction has been found to fit an approximately elliptical "cap model."[9] A cap model consists of a failure surface for a perfectly plastic material response, and an elliptic strain-hardening cap that extends isotropically about the hydrostatic axis[8]. A cap model consists of a failure surface for a perfectly plastic material response and an elliptic strain-hardening cap that extends isotropically about the hydrostatic axis.

The parametric equations of the failure envelope can be obtained by introducing the concept of poroelasticity, representing the state of stress by the effective mean stress (σ'_m) and the equivalent stress (σ_{eq}). In this work, we assumed the measurements (as well as the variables derive from them) are corrupted by experimental error We focused in triaxial tests for sedimentary rock like sandstone. To construct the envelope, we minimized the sum of the squares of the resulting distance by reconciling the measurements with the statistical method of error-in-variables, which assumes all the variables corrupted by experimental error. A nonlinear algebraic form represents the envelope equations delimiting the brittle/to/ductile transitional region of the failure or yield envelope. To illustrate the application of this methodology, we used the mechanical data for the brittle strength and compactive yield stress for Bentheim sandstone[43] and the normalized principal stresses describing brittle/ductile transition behavior for 10 different sandstones [44]. Our proposed methodology provides an accurate way of obtaining the parametric representation of the failure envelope, describing the deformation mechanism and indicates whether a given stress state will lead to failure or yield.

We use the statistical method of error-in-variables (EIV) to obtain the parametric representation of the failure envelope in the principal effective-stress plane; we assume that the proposed method provides an accurate way of obtaining the parametric representation of the failure envelope describing the deformation mechanism when considering pore collapse effect.

3.5.2. Methodology and procedure

Recalling that the state of stress can be represented by the equivalent stress $\left(\sigma_{eq}\right)$ and the effective mean stress $\left(\sigma'_{m}\right)$ with Eqs. 3-26 and 3-27, we can generate an algebraic solution for the material that will satisfy the equation of the envelope given in implicit form by Eq. 3-25.

The parametric representation proposed to fit the failure envelope in the principal effective stress plane is given by a four-parameter equation fitting the envelope in a way that describes the deformation mechanism by drawing a curve that connects the brittle region to the ductile region defining the cap model.

Then, Eq. 3-25 may be written as

$$h\left(\hat{\sigma}'_{mi}, \hat{\sigma}_{eqi}, \underline{\theta'''}\right) = \theta''_0 + \theta''_1\ \hat{\sigma}'_{mi} + \theta''_2\ \hat{\sigma}'^2_{mi} - \theta''_3\ \hat{\sigma}_{eqi} - \hat{\sigma}^2_{eqi} = 0 \ldots\ldots\ldots\ldots\ldots \quad (3\text{-}30)$$

3.5.3. Discussion and results

To illustrate how we used the EIV method to fit the envelope for a special model describing brittle/ductile transition with pore collapse effect in the principal effective-stress plane, we used the previously set experiments[43,44]. We assumed that a nonlinear parametric function fits the envelope. We obtained the failure envelopes for those rocks in the principal effective-stress plane, using all the available information. **Table 3-9** contains the optimal parameters for normalized data for 10 sandstones. The parameters describe the failure envelope located nearest to the respective pairs of the mean-effective and equivalent-stress measurements obtained from the data measured under various confining pressures for the critical pressure normalized data for 10 different sandstones. We obtained the standard deviation from the sum of the squared distances between the failure envelope and each pair of measurements (objective function values); the standard deviations result to be 0.06, which is given by

$$S.D = \sqrt{\frac{J}{n-4}} ,\dots\dots\dots\dots\dots\dots\dots\dots\dots\dots\dots\dots\dots\dots\dots\dots\dots\dots(3\text{-}31)$$

Fig. 3-12 shows the parametric representation of the envelope of the normalized principal stresses describing brittle/ductile transition behavior for 10 different sandstones. The solid black line represents the optimal parametric representation of the yield envelope.

        Table 3-10 contains the optimal parameters for Bentheim sandstone. The parameters describing the yield envelope located nearest to the respective pairs of the mean-effective and equivalent-stress measurements obtained from the measured data, including critical stress at the onset of dilatancy and compactive yield stress at the onset of shear-enhanced compaction (11 test samples) and considering only compactive yield stress defining a cap model (7 test samples). The standard deviation in this 12.2 MPa for

whole envelope and 10.2 MPa for the case when considering only compactive yield stress to define a cap model.

Figs. 3-13 shows the parametric representation of the envelope including critical stress at the onset of dilatancy and compactive yield stress at the onset of shear-enhanced compaction (11 test samples) and considering only compactive yield stress defining a cap model (7 test samples) for Bentheim sandstone. We should emphasize that according with some previous work a 400 MPa we have the critical pressure.

3.5.4. Conclusions

The EIV method can introduce a reliable way to draw the parametric representation of the envelope in the principal effective-stress plane for the deformation mechanism describing a cap model in the case when the tested rock is affected by pore-collapse.

TABLE 3-9- OPTIMAL PARAMETERS DETERMINED FROM THE EIV METHOD CONSIDERING PORE COLLAPSE EFFECT FOR A NORMALIZED DATA

	Nonlinear 4 Parameters model			
	$f\left(\hat{\sigma}'_m, \hat{\sigma}_{eq}, \underline{\theta}''\right) = \theta''_0 + \theta''_1\hat{\sigma}'_m + \theta''_1\hat{\sigma}'^2_m - \theta''_3\hat{\sigma}_{eq} - \hat{\sigma}_{eq}^2$			
	θ_0	θ_1	θ_2	θ_3
Test rock	MPa^2	MPa	(-)	MPa
Normalized data from 10 sandstones	5.1E-13	20.7	-18.2	10.4

 35 Test samples
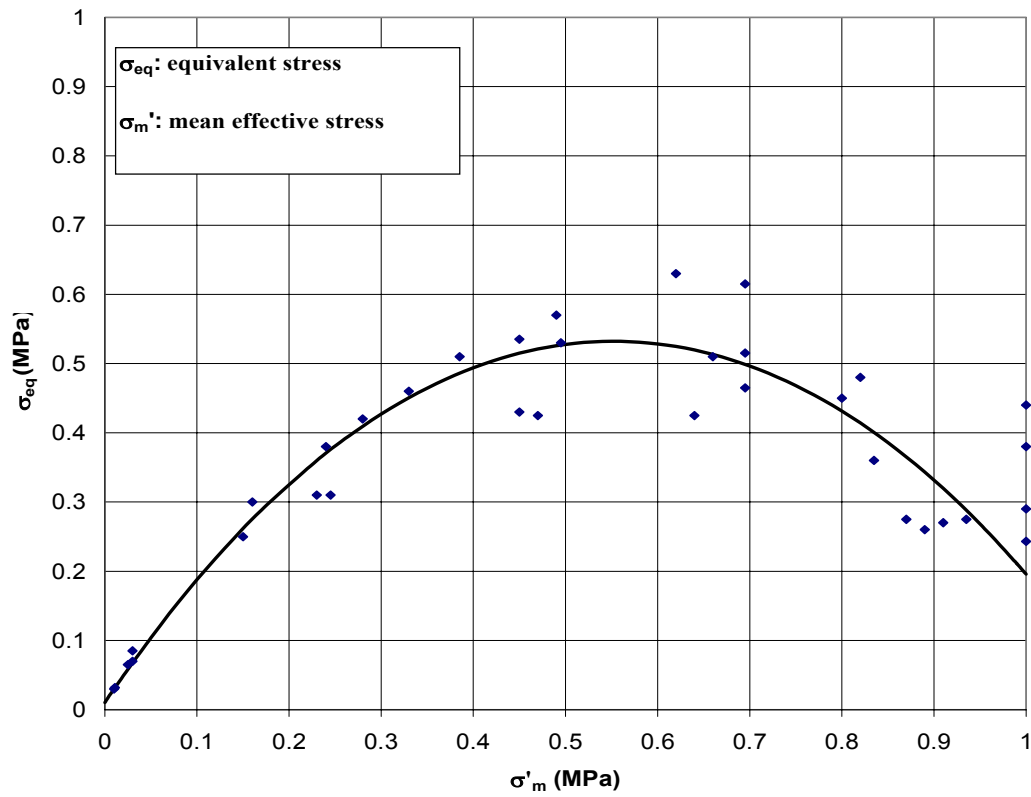
Fig. 3-12-   Parametric representation of the failure envelope in the principal stress plane considering pore collapse effect using EIV method for normalized data for 10 sandstones (Nonlinear four-parameters model)

TABLE 3-10- OPTIMAL PARAMETERS DETERMINED FROM THE EIV METHOD FOR BENTHEIM SANDSTONECONSIDERING PORE COLLAPSE EFFECT

	Nonlinear 4 Parameters model			
	$f(\hat{\sigma}_m,\hat{\sigma}_e,\underline{\theta''})=\theta''_0+\theta''_1\hat{\sigma}_m+\theta''_1\hat{\sigma}_m^2-\theta''_3\hat{\sigma}_e-\hat{\sigma}_e^2$			
	θ''_0	θ''_1	θ''_2	θ''_3
Test rock	MPa^2	MPa	(-)	MPa
Bentheim sandstone[a]	7.9E-13	1717.4	-3.7	652
Bentheim sandstone[b]	1.4E+5	629.6	-1.9	562.4

a: 11 Test samples
b: 7 Test samples
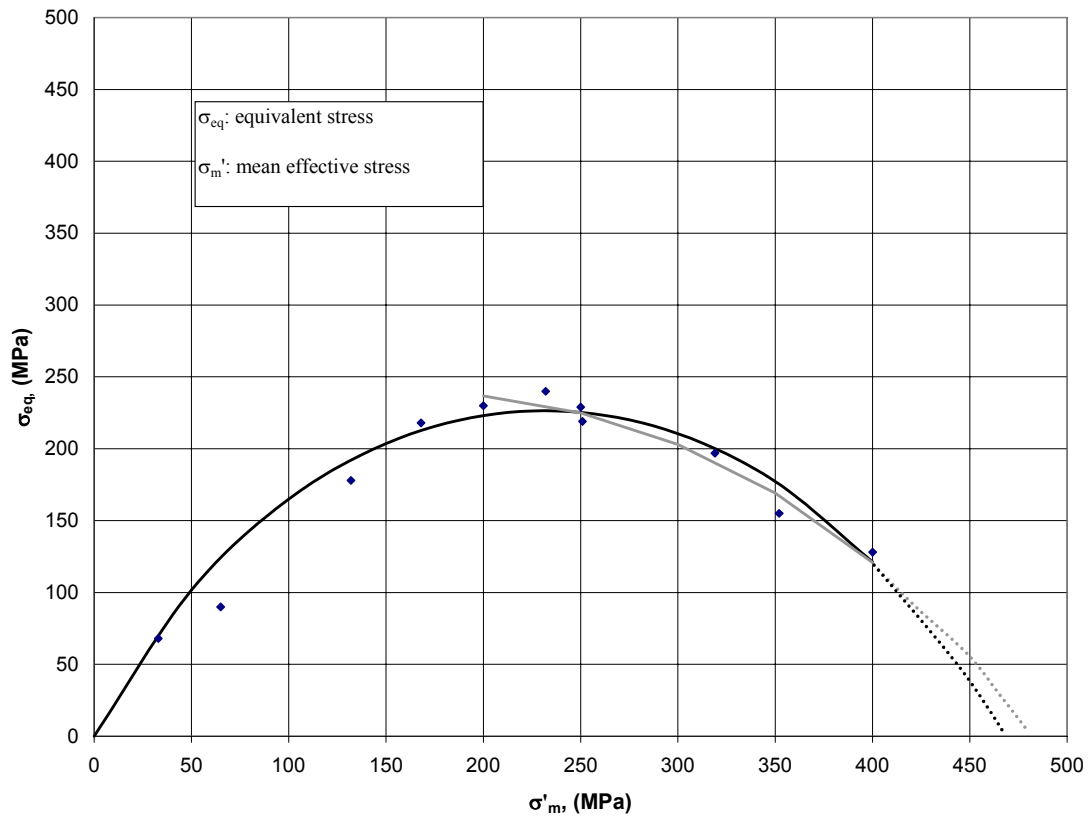
Fig. 3-13-   Parametric representation of the failure envelope in the principal stress plane considering pore collapse effect using EIV method for Bentheim sandstone (Nonlinear four-parameters model) . Based on conventional triaxial test data .

CHAPTER IV

FITTING PARAMETRIC MODELS IN 3D

4.1. Introduction

This chapter contains the application of the statistical based method of error-in-variables (EIV) to obtain the parametric representation of a failure surface in 3D. The developed methodology used to fit the failure envelope in 2D is extended into the stress space considering the influence of the intermediate principal stress. Data from "true" triaxial tests[23] are used to represent the failure surface directly in the principal stress space. Because we had already demonstrated that the EIV method, which assumes that all variables having experimental error, provides a better representation of the failure envelope than the previously proposed methodology for 2D models we provide an extension of this methodology to 3D models using an established set of "true" triaxial data.[23]

We restrict this work to the processing of data obtained in "true" triaxial experiments conducted in homogenous, isotropic rock at isothermal conditions. Even though sedimentary rocks like sandstone are the focuses of this study because of their importance in near-wellbore reservoir rock stability problems; the proposed methodology is not limited to this type of rock. To simplify the understanding of the application of this methodology in the principal stress space, we consider only experimental data containing the compressive region of the stress state for the selected 3D models.

Two 3D parametric models (elliptic cone and elliptic paraboloid) are proposed to represent the failure surface in the principal stress space, because of their simplicity.

4.2. Fitting failure surface in the principal stress space.

4.2.1. Introduction

Assuming that the intermediate principal stress influences rock strength, a failure criterion may be expressed in terms of the major (σ_1), intermediate (σ_2) and minor (σ_3) principal stresses $[\sigma_1 > \sigma_2 > \sigma_3]$ with compression positive.

$$g(\sigma_1, \sigma_2, \sigma_3) = 0 \dots\dots\dots\dots\dots\dots\dots\dots\dots\dots\dots\dots\dots\dots\dots\dots\dots\dots\dots(4\text{-}1)$$

Most of the empirical failure criteria have been formulated in terms of σ_1 and σ_3 being independent of σ_2, however, Pan and Hudson[25] reviewed several criteria, which include the influence of the intermediate principal stress and proposed a 3D variation of the Hoek and Brown criterion[21]. Wang and Kemeny[26] modify Beiniawiski's equation, which is based on hollow cylinder test results of three types of rocks. Sheorey[23] provides a list of the most relevant empirical failure equations.

The least-squares method has been widely adopted to fit the failure envelope directly from the experimental data. Mostyn and Douglas[22] presented different results fitting the different forms of the Hoek and Brown[21] criterion.

We extend the EIV approach to the principal stress space. To determine the conditions, which govern fracture of rock, a general three-dimensional failure criterion is required, so the state of stress in the field needs to be determined in all three dimensions. In this case we will obtain a parametric equation for the failure surface.

4.2.2. Methodology and procedure

The 3D model may be written in its implicit form as:

$$g(\hat{\sigma}_1, \hat{\sigma}_2, \hat{\sigma}_3, \underline{\theta'}) = 0 \ \dots\dots\dots\dots\dots\dots\dots\dots\dots\dots\dots\dots\dots\dots\dots\dots\dots(4\text{-}2)$$

To obtain the optimal parameters of the parametric representation of the failure surface we must minimize the sum of the squared distance given by the relation

$$J = \sum_{i=1}^{n} d_{p_i}^2 \ \dots\dots\dots\dots\dots\dots\dots\dots\dots\dots\dots\dots\dots\dots\dots\dots\dots(4\text{-}3)$$

where for each pair of measurements

$$d_{p_i}^2 = (\hat{\sigma}_{1i} - \sigma_{1i})^2 + (\hat{\sigma}_{2i} - \sigma_{2i})^2 + (\hat{\sigma}_{3i} - \sigma_{3i})^2 \ \dots\dots\dots\dots\dots\dots\dots\dots\dots(4\text{-}4)$$

Because a surface represents the limit between stable and unstable zones of the stress state in principal stress space, we define an algorithm in terms of the perpendicular line to the tangent plane of the surface and each measured point using EIV, which considers the shortest distance to reconcile each point to the failure surface. The derivation of the equations and the selected models appear in Appendix B.

4.2.3. Discussion and results

To illustrate and verify the applicability of the statistics-based method of error-in-variables to obtain the parametric representation of the failure surface in the principal-stress space the results of previous polyaxial tests for Shirahama, Izumi and Horonai sandstones is used[23] assume elliptic cone and elliptic paraboloid models. Our goal is to obtain all the optimum failure surfaces for the three rocks, using all the available information.

The selected data consist of "true" triaxial measurements from a series of compressive tests reported by Takahi and Koide (1989) and compiled by Sheorey.[23] There are 42, 23 and 31 measurements for Shirahama, Izumi and Horonai sandstone

respectively. The objective function for each rock was minimized to obtain the best fit with the selected models. **Table 4-1** contains the optimal parameters for the elliptic cone and elliptic paraboloid models for each of the selected rocks. The possible use of these parameters is within a computational algorithm, where a stress state needs to be tested for failure. Using the listed parameters, we can minimize the likelihood of making a wrong judgment (i.e. declaring a failure state as safe or a safe state as failure.)

The standard deviation is obtained from the sum of the squared distances between the failure surface and each of the measured points (objective function values, **Table 4-2**). This particular application of the statistics-based method of error-in-variables is limited to the case where the data are obtained in the compression region. We use no the tensile strength data. In addition, we force the failure surface to cross the origin of coordinates to provide a clear physical interpretation without restriction of our general approach. This limitation that may be removed in future research. Another way to represent the data in 3D is using the invariant of the stress deviator tensor. We can plot the data in 2D considering that $I_1 = \sigma_1 + \sigma_2 + \sigma_3$ represent the first invariant and,

$J_2 = \dfrac{1}{6}\left[(\sigma_1 - \sigma_2)^2 + (\sigma_1 - \sigma_3)^2 + (\sigma_2 - \sigma_3)^2\right]$ is the second invariant of deviatoric stress.

$\dfrac{I_1}{3}$ vs $\sqrt{3J_2}$ for Shirahama sandstone is shown in **Fig. 4-1** as an example.

4.2.4. Conclusions

The EIV method provides a new and efficient methodology to fit experimental data and obtain the parametric representation of the failure surface in 3D principal stress space.

TABLE 4-1- OPTIMAL PARAMETERS DETERMINED FROM EIV METHOD FOR THE FAILURE SURFACE IN THE PRINCIPAL STRESS SPACE

	Elliptic Cone			Elliptic Paraboloid		
	$f(\hat{\sigma}_3,\hat{\sigma}_2,\hat{\sigma}_1,\underline{\theta'}) = \theta_1'^2\hat{\sigma}_3^2 + \theta_2'^2\hat{\sigma}_2^2 - \theta_3'^2\hat{\sigma}_1^2$			$f(\hat{\sigma}_3,\hat{\sigma}_2,\hat{\sigma}_1,\underline{\theta'}) = \theta_1'^2\hat{\sigma}_3^2 + \theta_2'^2\hat{\sigma}_2^2 - \theta_3'\,\hat{\sigma}_1$		
	θ_1	θ_2	θ_3	θ_1	θ_2	θ_3
Test rock	(-)	(-)	(-)	(-)	(-)	(-)
Shirahama sandstone[a]	32.1	0.2	4.3	0.6	4.2E-6	1.2
Izumi sandstone[b]	62.1	0.3	4.3	0.3	2.1E-6	0.2
Horonai sandstone[c]	40.4	2.2E-8	4.3	0.09	4.0E-7	0.02

a: 42 Test samples
b: 23 Test samples
c: 31 Test samples

TABLE 4-2- STANDARD DEVIATION BETWEEN EACH MEASURED POINT AND FAILURE SURFACE FROM EIV METHOD IN THE PRINCIPAL STRESS SPACE

	Elliptic Cone	Elliptic Paraboloid
	$f(\hat{\sigma}_3,\hat{\sigma}_2,\hat{\sigma}_1,\underline{\theta'}) = \theta_1'^2\hat{\sigma}_3^2 + \theta_2'^2\hat{\sigma}_2^2 - \theta_3'^2\hat{\sigma}_1^2$	$f(\hat{\sigma}_3,\hat{\sigma}_2,\hat{\sigma}_1,\underline{\theta'}) = \theta_1'^2\hat{\sigma}_3^2 + \theta_2'^2\hat{\sigma}_2^2 - \theta_3'\,\hat{\sigma}_1$
	EIV	*EIV*
Test rock	(%)	(%)
Shirahama sandstone[a]	10.9	14.1
Izumi sandstone[b]	6.5	9.1
Horonai sandstone[c]	9.8	12.7

a: 42 Test samples
b: 23 Test samples
c: 31 Test samples
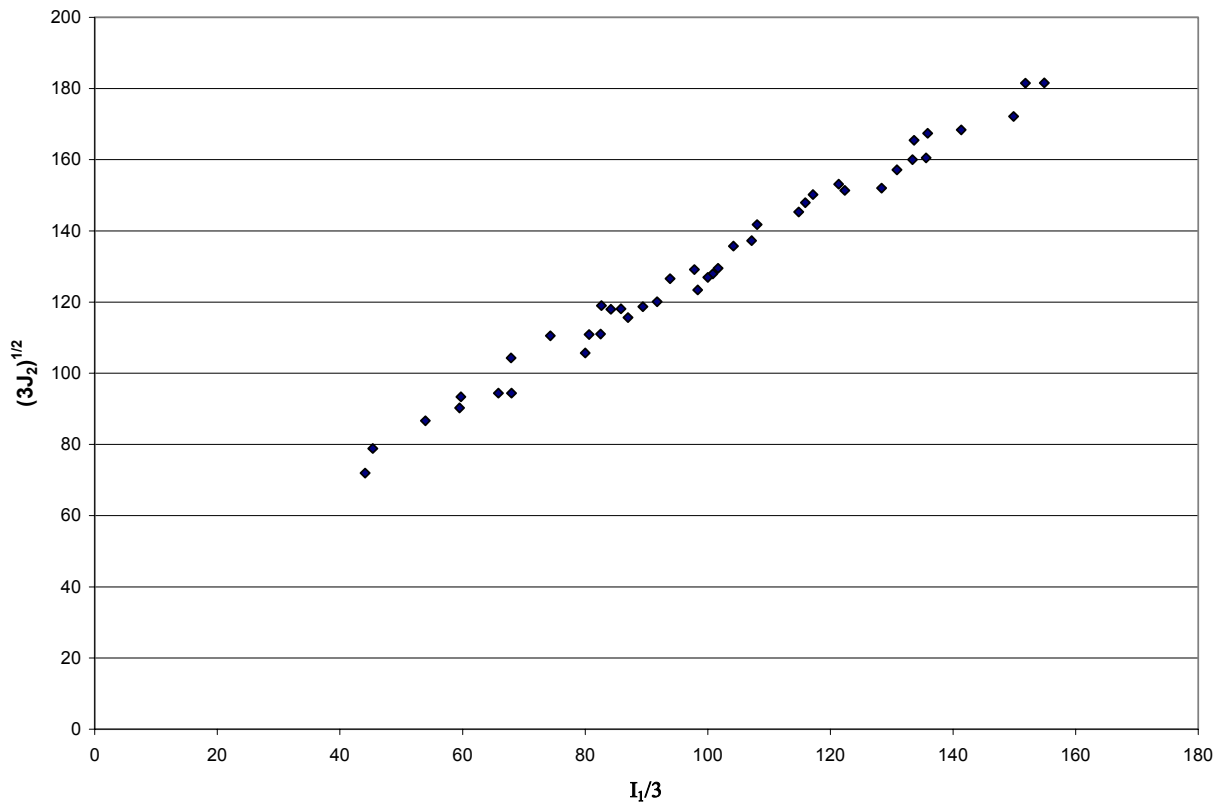
Fig. 4-1- $(3J_2)^{1/2}$ vs $I_1/3$ for Shirahama Sandstone.

CHAPTER V

SUMMARY, CONCLUSIONS AND RECOMMENDATIONS

An improvement in the parametric representation of failure criteria used to characterize rock strength of a reservoir rock in the near-wellbore region has been addresses in this study. A statistical technique, the error-in-variables (EIV) method, has been adopted in our work. This method takes into account experimental errors in all the measured variables. The parametric equations have been obtained both in the plane (2D) and the space (3D) geometries.

The following conclusions can be derived from the present research:

- The EIV procedure can be applied to virtually any failure-envelope model. It provides exactly reproducible envelope parameters from a given set of data.
- The resulting parameters correspond to a well-defined optimality criterion that makes more statistical and rock-mechanical sense than the traditional least-squares approach because the EIV method accounts for measurement errors in all variables.
- The smoothness (differentiability) of the resulting envelope makes it suitable for use in applications requiring differentiable failure function. Interpolation within the range of the envelope equation can be done more accurately than with segmented representations for the nonlinear models.
- EIV method shows improvement for the parametric representation of the failure envelope in the principal stress plane. The transformation process from the principal stress plane to the Mohr plane, can provide at least one case a more

appropriate and accurate approximation than those obtained when fitting the failure envelope directly in the Mohr plane.

- The statistics-based EIV method improves methodology to obtain the parametric representation of the envelope in the principal stress plane when considering the pore-pressure influence describing a more appropriate form of the deformation mechanism for the tested rock.

- The EIV method introduced a reliable way to construct the yield envelope in the effective-stress plane in the case when the tested rock is affected by pore-collapse.

- The parametric representation of the failure criteria in the near-wellbore region of reservoir rock could serve as a base for further studies in problems such as borehole stability, propensity for sanding as well as subsidence, which is related to the pore collapse effect.

NOMENCLATURE

a = tangent vector to the envelope at $(\hat{\sigma}_i, \hat{\tau}_i)$

a = tangent vector to the envelope at $(\hat{\sigma}_{3i}, \hat{\sigma}_{1i})$

a = tangent vector to the envelope at $(\hat{\sigma}'_{mi}, \hat{\sigma}_{eqi})$

b = vector starting from the center of the Mohr's circle and ending at $(\hat{\sigma}_i, \hat{\tau}_i)$

b = vector from the measured i-th point to the envelope

c_i = center of the i-th Mohr's circle

CFM = closed-form model

d_i = geometric distance in EIV method in Mohr plane

d_{iLS} = "vertical" distance in least squares method.

$\dfrac{\partial g()}{\partial \sigma_k}$ = gradient

d_{pi} = geometric distance in EIV method

EIV = error-in-variables

$f()$ = parametric function

$\tilde{f}()$ = parametric function

$g()$ = parametric function

$h()$ =parametric function

I_1 =first stress invariant

J =sum of square distance

J_2 =second invariant of the stress tensor

k =proportional distance from the measured points to the surface.

LS =least-square

P_j=interception point

r_i =radius of the i-th Mohr's circle

x_i =measured value of the abscissa

x =constant

y =constant

y_i =measured value of the ordinate

$\hat{y}_{iLS}$ =calculated value of the ordinate from least square

$\hat{x}_i$ =reconciled value of the abscissa from EIV

$\hat{y}_i$ =reconciled value of the ordinate from EIV

Greek letters

σ_{1i} =i-th measured axial stress

σ_{3i} =i-th measured lateral stress

σ_{1i} =$i\text{-}th$ measured major principal stress

σ_{2i} =$i\text{-}th$ measured intermediate principal stress

σ_{3i} =$i\text{-}th$ measured minor principal stress

$\hat{\sigma}_{1i}$ =$i\text{-}th$ reconciled major principal stress

$\hat{\sigma}_{2i}$ =$i\text{-}th$ reconciled intermediate principal stress

$\hat{\sigma}_{3i}$ =$i\text{-}th$ reconciled minor principal stress

σ'_{mi} =$i\text{-}th$ derived mean effective stress

σ_{eqi} =$i\text{-}th$ derived equivalent stress

$\hat{\sigma}'_{mi}$ =$i\text{-}th$ reconciled mean effective stress

$\hat{\sigma}_{eqi}$ =$i\text{-}th$ reconciled equivalent stress

σ_i =calculated normal stress of $i\text{-}th$ Mohr circle

$\hat{\sigma}_i$ =reconciled normal stress of $i\text{-}th$ Mohr circle

τ_i =calculated shear stress of $i\text{-}th$ Mohr circle

$\hat{\tau}_i$ =reconciled shear stress of $i\text{-}th$ Mohr circle

$\underline{\theta}$ =vector of unknown parameters in the Mohr plane

$\underline{\theta}'$ =vector of unknown parameters in the principal-stress plane or space

REFERENCES

1. Paterson, M. A.: *Experimental Rock Deformation: The Brittle Field*, Springer-Verlag, New York (1978).

2. Evans, B., Fredrich, J. T. and Wong, T.: "The Brittle-Ductile Transition in Rocks: Recent Experimental and Theoretical Progress," *American Geophysical Union Geophysical Monograph* **56**, Washington DC,(1990) 1-20.

3. Handin, J. "*Handbook of Physical Constants, Strength and Ductility*" *Geol. Soc. Amer. Memoir* (1966), **97**, 238.

4. Terzagui, K.: *Theoretical Soil Mechanics*, Wiley, New York (1943).

5. Nur, A. and Byerlee, J.D.: "An Exact Effective Stress Law for Elastic Deformation of Rock with Fluids," *J. of Geophys. Res.*, (1971), **76**, 6414.

6. Addis, M. A.: "Material Metastability in Weakly Cemented Sedimentary Rocks," *Memoir of the Geological Society of China*, (1987), **9**, 495.

7. Smits, R. M., de Wall, J. A. and van Kooten, J. F. C.: " Prediction of Abrupt Reservoir Compaction and Surface Subsidence caused by Pore Collapse in Carbonates," *SPEFE* (March 1988), 340.

8. Wong, T. E., David, C. and Zhu, W.: "The Transition From Brittle Faulting to Cataclastic Flow in Porous Sandstones: Mechanical Deformation," *J. of Geophys. Res.*, (1997), **102**, 3009.

9. Chen, W. F. and Mizumo, E.: *Nonlinear Analysis in Soil Mechanics: Theory and Implementation*, Elsevier Science, New York (1990).

10. Balmer, G. A.: "A General Analytical Solution for Mohr's Envelope," *Proc.*, ASTM (1952), **52**, 1260.

11. Pincus, H. J.: "Closed-Form/Least-Squares Failure Envelopes for Rock Strength," *Inter. J. of Rock Mechanics and Mining Sciences* (2000), **37**, 763.

12. Pincus, H. J.: "Interlaboratory Testing Program for Rock Properties, Round One-Longitudinal and Transverse Pulse Velocities, Unconfined Compressive Strength, Uniaxial Elastic Modulus, and Splitting Tensile Strength," *Geotechnical Testing J.* (1993), **16 (1)**, 138.

13. Pincus, H. J.: "Addendum to Interlaboratory Testing Program for Rock Properties, Round One," *Geotechnical Testing J.* (1994), **17** No 2, 256.

14. Pincus, H. J.: "Interlaboratory Testing Program for Rock Properties, Round Two-Confined Compression: Young's Modulus, Poisson's Ratio, and Ultimate Strength," *Geotechnical Testing J.* (1996), **19** No 3, 321.

15. Griffith, A. A.: "The Phenomena of Rupture and Flow in Solids" *Phil. Trans. Roy. Soc., London*, (1921), **A 221**, 163-198.

16. Zhou, S.: 'A Program to Model the Initial Shape and Extent of Borehole Breakout," *Computer & Geos.* (1994), **20** No 7/8, 1143.

17. Lade, P.: " Elasto-Plastic Stress-Strain for Cohesionless Soil with Curved Yield Surfaces," *International Journal of Solids and Structures* (1977), **13**, 1019.

18. Drucker, D. and Prager, W.: "Soil Mechanics and Plastic Analysis or Limit Design," *Q. Appl. Math.* (1952), **10**, 157.

19. Murrel, S. A. F.: "A Criterion for Brittle Fracture of Rocks and Concrete Under Triaxial Stress and the Effect of Pore Pressure on the Criterion," *Proc.* Fifth Rock Mechanics Symposium, University of Minnesota, in Rock Mechanics, C. Fairhurst (Ed.), Oxford, Pergamon (1990) 563-577.

20. Hobbs, D. W.: "The Strength and the Stess-Strain Characteristics of Coal in Triaxial Compression," *J. Geol*. (1964), **72**, 214.

21. Hoek, E. and Brown, E. T.: Underground Excavation in Rock, The Institution of Mining and Metallurgy, London (1980).

22. Mostyn, G. and Douglas, K.: "Strength of Intact Rock and Rock Masses," http://geotle.t.u-tokyo.ac.jp/towhata/lecture/rock/mostyn.pdf, 1 August 2002.

23. Sheorey, P. R.: *Empirical Rock Failure Criteria* A.A.Balkema, Rotterdam, The Netherlands, (1997).

24. Mogi, K.: "Presure Dependence of Rock Strength and Transition from Brittle Fracture to Ductile Flow," *Bulletin of Earthquake Research Institute*, University of Tokyo (1966), **44** No 1, 215.

25. Pan, X. D. and Hudson, J. A.: "A Simplify Three-Dimensional Hoek-Brown Yield Criterion," *Rock Mechanics and Power Plants* Ed. M. Romana (1988) v 1, Balkema, Rotterdam,The Netherlands, 95.

26. Wang, R. and Kemeny, J. M.: " A New Empirical Failure Criterion for Rock Under Polyaxial Compressive Stresses," *35ᵗʰ US Symp. Rock Mech.* Eds. J.J.K. Daemen and R. A. Schultz (1995), Balkema, Rotterdam, 453.

27. Biot, M. A.: "General Theory of Three-Dimensional Consolidation," *J. of Appl. Phys*., (1941), **12**, 182.

28. Jaeger, J. C. and Cook, N. G. W.: *Fundamentals of Rock Mechanics* Halsted Press, New York 1979.

29. Deming, W. E.: *Statistical Adjustment of Data,* Willey, New York, (1943).

30. York, P.: "Least Squares Fitting a Straight Line," *Can. J. Phys.* (1966), **44**, 1708.

31. Willians, J. H.: Least Squares Fitting of a Straight Line," *Can. J. Phys.* (1968), **45**, 1845.

32. O' Neil, M., Sinclair, I. G. and Smith, F. J.: "Polynomial Curve Fitting When Abscissas and Ordinates Are Both Subject to Error," *Computer J.* (1969), **12**, 52.

33. Southwell, W.H.: "Fitting Experimental Data," *J. Comput. Phys.* (1969), **4**, 465.

34. Britt, H. I. and Luecke, R. H.: "The Estimation of Parameters in Nonlinear, Implicit Models," *Technometrics* (1973), **15**, 233.

35. Peneloux, A.R., Deyrieux, E. and Neau, E.: "The Maximum Likelihood Test and the Estimation of Experimental Inaccuracies: Application to Data Reduction for Vapor-Liquid Equilibrium," *J. de Phys.* (1976), 706.

36. Reilly, P. M. and Patino-Leal, H. A.: "Bayesian Study of the Error-in-Variables Model," *Technometrics* (1981), **23** No 3, 221.

37. Schwetlick, H. and Tiller, V.: "Numerical Methods for Estimating Parameters in Nonlinear Models with Error in the Variables," *Technometrics* (1985), **27** No 1, 17.

38. Valkó, P. and Vajda, S.: "An Extended Marquardt-Type Procedure for Fitting Error-in-Variables Models," *Computational Chemical Eng.* (1987), **11** No 1 , 37.

39. Liebman, M. J. and Edgar, T. F.: "Data Reconciliation for Nonlinear Processes," *Preprint, AIChE Annual. Meeting*, Washington, DC. (1988).

40. Edgar, T. F., Liebman, M. J. and Kim, I. W.: "Robust Error-in-Variables Estimation Using Nonlinear Programming Techniques," *AIChE J.* (1990), **v 36** No 7, 985.

41. Esposito, W. R. and Floudas, C. A.: "Parameter Estimation in Nonlinear Algebraic Models via Global Optimization," *Computers and Chemical Eng.* (1998), **22**, Suppl., S213-220.

42. Aldrich, M.J.: "Pore Pressure on Berea sandstone Subjected to experimental Deformation," *Geol. Soc. Amer.* (1969), Bulletin 80, 1577.

43. Zhang, J.J., Rai, C.S. and Sondergeld, C.H.: "Mechanical Strength of Reservoir Materials: Key Information for Sand Prediction," *SPE Reservoir Eval & Eng.* (2000), **3** No 2, 127

44. Klein, E., Baud, P., Reuschlé T. and Wong, T.: "Mechanical Behaviour and Faliure Mode of Bentheim Sandstone Under Triaxial Compression," *Phys. Chem earth (A)* (2001), **26** No (1-2**)**, 21.

45. Zambrano-Mendoza, O., Valkó, P.P. and Russell, J. E.: "Error-in-Variables for Rock Failure Envelope," *Inter. J. of Rock Mechanics and Mining Sciences* (2002), Rock Mechanics and Mining Sciences 1152, in press.

APPENDIX A

DERIVATION OF THE PARAMETRIC REPRESENTATION FOR FAILURE CRITERIA IN 2D

Introduction

The objective of this appendix is to present the methodology to obtain the parametric representation of the failure envelope using the error-in-variables (EIV) method. Likewise, we developed a methodology to transform the EIV, resulting in a parametric representation in the principal stress plane and, in the Mohr plane. The following systematic mathematical derivations are presented in this appendix:

1. Fitting-failure envelope in the Mohr plane,
2. fitting-failure envelope in the principal stress plane,
3. fitting-failure envelope including poroelastic effect, applying the method to special models suitable for describing brittle/ductile transition in the yield envelope;
4. and the Balmer's-method-based generalization to obtain a parametric representation in the Mohr plane from the representation in the principal-stress plane.

Fitting failure envelope directly in the Mohr plane

Typically, a failure criterion is expressed in terms of the major σ_1 and minor σ_3 principal stresses; and for this reason, for every stress state (σ_3, σ_1) producing a failure during the triaxial failure experiments, a Mohr circle can be drawn on the σ, τ plane according to Eq. A-1:

$$\left(\sigma - \left(\frac{\sigma_1 + \sigma_3}{2}\right)\right)^2 + \tau^2 = \left(\frac{\sigma_1 - \sigma_3}{2}\right)^2 \ \text{...} \text{(A-1)}$$

The failure envelope is then defined as the curve enveloping (touching from one side) all these circles. The equation of the failure envelope can be represented by Eq. A-2:

$$f(\sigma, \tau) = 0 \ \text{...} \text{(A-2)}$$

Application of EIV method to fit failure envelope in the Mohr plane

In the Mohr plane, the EIV method should be modified to apply to the failure-envelope problem, because a circle, not a point, represents the measurements. The generalization of the EIV method is straightforward, once the concept of distance is interpreted. Shown in **Fig. A-1** shows two Mohr's circles and the failure envelope.

For circle one, the distance of the Mohr circle from the envelope is denoted by d_1 as shown in **Fig. A-1**. Circle 2 intercepts the envelope and its distance from the curve, d_2, is defined as the distance of the furthest point P_2 of the circle, lying in the unstable half plane. The engineering interpretation is that we have to modify the radius of the observed Mohr circle by distances d_1 or d_2 to reconcile the measurement with the envelope. Obviously, our goal is to minimize the sum of squares of distances, d_i:

$$J = \sum_{i=1}^{n} d_i^2 \ \text{..} \text{(A-3)}$$

The reconciled stress state satisfies the equation of the envelope:

$$f(\hat{\sigma}_i, \hat{\tau}_i, \underline{\theta}) = 0 \ \text{...} \text{(A-4)}$$

Introducing the "observed" radius

$$r_i = \frac{\sigma_{1i} - \sigma_{3i}}{2} \quad \dots\dots\dots\dots\dots\dots\dots\dots\dots\dots\dots\dots\dots\dots\dots\dots \quad (A-5)$$

and center

$$c_i = \frac{\sigma_{1i} + \sigma_{3i}}{2} \quad \dots\dots\dots\dots\dots\dots\dots\dots\dots\dots\dots\dots\dots\dots\dots \quad (A-6)$$

we can express the distance as

$$d_i^2 = \left(\sqrt{(c_i - \hat{\sigma}_i)^2 + \hat{\tau}_i^2} - r_i \right)^2 \quad \dots\dots\dots\dots\dots\dots\dots\dots\dots\dots\dots\dots \quad (A-7)$$

Substituting Eq. A-7 into A-3 we obtain

$$J = \sum_{i=1}^{n} \left(\sqrt{(c_i - \hat{\sigma}_i)^2 + \hat{\tau}_i^2} - r_i \right)^2 \quad \dots\dots\dots\dots\dots\dots\dots\dots\dots\dots\dots\dots \quad (A-8)$$

Then minimizing Eq. A-8 subject to the constraint of Eq. A-4 constitutes the EIV formulation.

The sum of squared distance in Eq. A-8 could be weighed expressing the sum of the squared distance relative to the radius of each of the circles as follows:

$$J = \sum_{i=1}^{n} \left[\frac{\left(\sqrt{(c_i - \hat{\sigma}_i)^2 + \hat{\tau}_i^2} - r_i \right)}{r_i} \right]^2 \quad \dots\dots\dots\dots\dots\dots\dots\dots\dots\dots\dots\dots \quad (A-9)$$

Because of the simple form of the objective function in Eq. A-8, the following algorithm can be used.
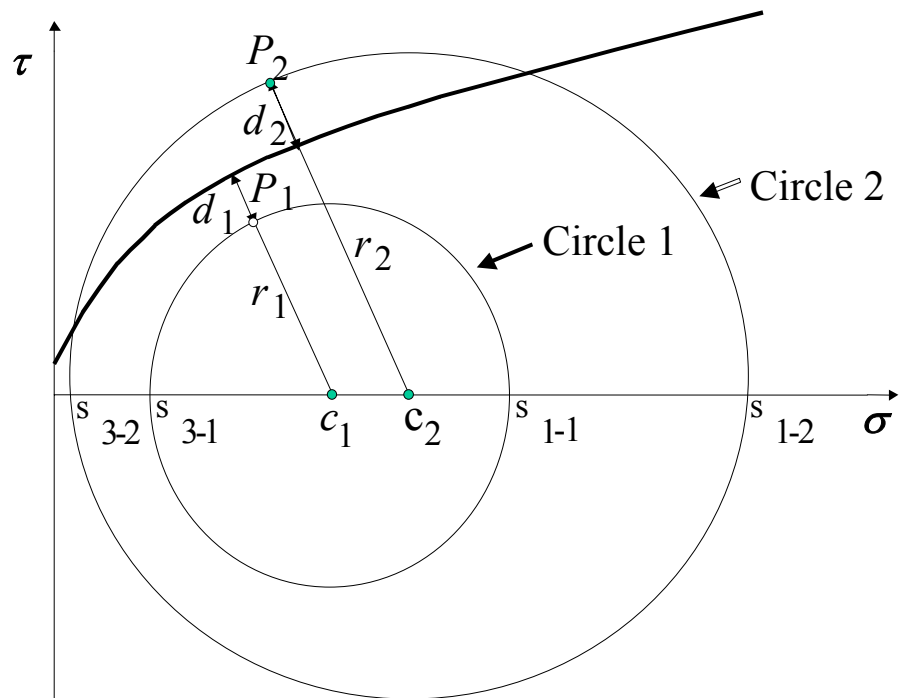
Fig A-1- Schematic representation of the error-in-variables approach applied to failure envelope determination in Mohr plane.
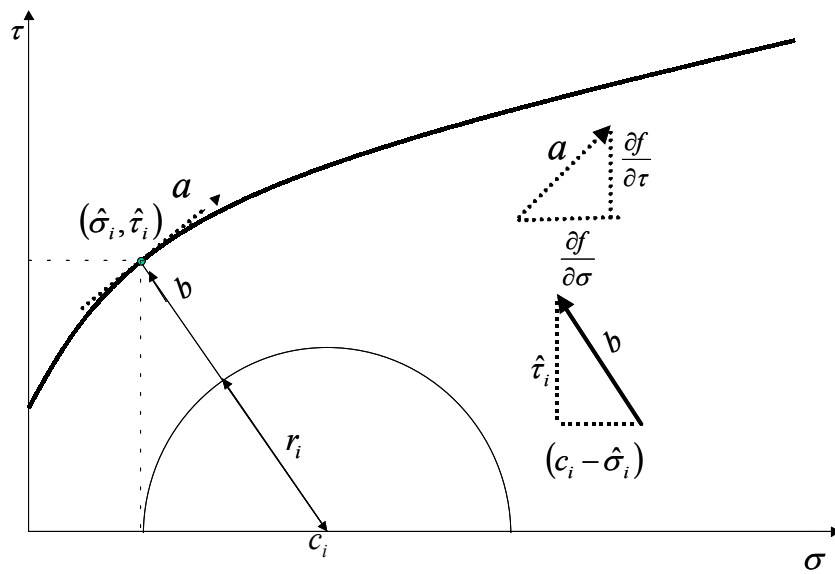
Fig. A-2- Graphic representation of the EIV algorithm in the Mohr plane.

Error-in-variables algorithm applied to the Mohr plane

Fig. A-2 illustrates the way to reconcile the measured points using the EIV approach.

Let a, denote the tangent vector of the envelope at $(\hat{\sigma}_i, \hat{\tau}_i)$

$$a = -\frac{\partial f(\hat{\sigma}_i, \hat{\tau}_i, \underline{\theta})}{\partial \hat{\tau}} i + \frac{\partial f(\hat{\sigma}_i, \hat{\tau}_i, \underline{\theta})}{\partial \hat{\sigma}} j \quad \dots\dots\dots\dots\dots\dots\dots\dots\dots\dots\dots\dots\dots\text{(A-10)}$$

and b the vector from the center of the *i-th* circle to the envelope:

$$b = (c_i - \hat{\sigma}_i) i + \hat{\tau}_i j \quad \dots\dots\dots\dots\dots\dots\dots\dots\dots\dots\dots\dots\dots\dots\dots\text{(A-11)}$$

From EIV a and b must be orthogonal each other, then $a \cdot b = 0$:

$$-(c_i - \hat{\sigma}_i)\frac{\partial f(\hat{\sigma}_i, \hat{\tau}_i, \underline{\theta})}{\partial \hat{\tau}} + \hat{\tau}_i \frac{\partial f(\hat{\sigma}_i, \hat{\tau}_i, \underline{\theta})}{\partial \hat{\sigma}} = 0 \quad \dots\dots\dots\dots\dots\dots\dots\dots\dots\text{(A-12)}$$

At any parameter vector $\underline{\theta}$, the system of Eqs. A-4 and A-12 can be solved simultaneously to obtain $(\hat{\sigma}, \hat{\tau})$, and hence the objective function can be evaluated.

For the three most frequently used envelope equations, the solutions are given as follows.

Application to selected models

Linear envelope equation

For this case, Eq. A-4 can be expressed as

$$f(\hat{\sigma}_i, \hat{\tau}_i, \theta) = \theta_0 + \theta_1 \hat{\sigma}_i - \hat{\tau}_i = 0 ,\dots\dots\dots\dots\dots\dots\dots\dots\dots\text{(A-13)}$$

where, θ_0 and θ_1 are the parameters of the linear envelope. Eq. A-12 can be represented as

$$c_i - \hat{\sigma}_i - \theta_1 \hat{\tau}_i = 0 \dots\dots\dots\dots\dots\dots\dots\dots\dots\text{(A-14)}$$

Solving the system of Eqs. A-13 and A-14 the solution for the squared distance is

$$d_i^2 = \left(\sqrt{\frac{(\theta_0 + c_i \theta_1)^2}{1 + \theta_1^2}} - r_i \right)^2 \dots\dots\dots\dots\dots\dots\dots\text{(A-15)}$$

Substituting Eq. A-15 into the objective function of Eq. A-8 we arrive at an unconstrained minimization problem involving two unknown parameters: θ_0 and θ_1. For this works, we programmed the objective functions in Visual Basic and used the GRG2 optimization code ("Solver") available in Microsoft-Excel. The starting point of the iterative minimization was obtained by traditional (generalized) least-squares (that is, artificially creating "independent" and "dependent" variables).

Parabolic envelope equation

For the parabolic approximation of the envelope, Eq. A-4 can be written as

$$f(\hat{\sigma}_i, \hat{\tau}_i, \theta) = \theta_0 + \theta_1 \hat{\sigma}_i - \hat{\tau}_i^2 = 0 \dots\dots\dots\dots\dots\dots\dots\text{(A-16)}$$

where θ_0 and θ_1 are the parameters. The appropriate form of Eq. A-12 is

$$[2(\hat{\sigma}_i - c_i) + \theta_1] \hat{\tau}_i = 0 \dots\dots\dots\dots\dots\dots\dots\text{(A-17)}$$

Solving the system of Eqs. A-16 and Eq. A-17, we obtain

$$d_i^2 = \left(\sqrt{\theta_0 + c_i\theta_1 - \frac{\theta_1^2}{4}} - r_i \right)^2 \quad \text{..} \quad \text{(A-18-a)}$$

Except for the degenerate case of the squared distance, d_i^2 can be expressed

$$d_i^2 = \left(\sqrt{\left(\frac{\theta_0}{\theta_1} + c_i \right)^2} - r_i \right)^2 \quad \text{..} \quad \text{(A-18-b)}$$

Hyperbolic envelope equation

For a hyperbolic, two-parameter model:

$$f(\hat{\sigma}_i, \hat{\tau}_i, \theta) = \theta_0 + \theta_1\hat{\sigma}_i^2 - \hat{\tau}_i^2 = 0 \quad \text{..} \quad \text{(A-19)}$$

Eq. A-12 takes the form

$$\left[2(\hat{\sigma}_i - c_i) + 2\theta_1\hat{\sigma}_i \right]\hat{\tau}_i = 0 \quad \text{..} \quad \text{(A-20)}$$

Solving the system of Eqs. A-19 and A-20, the squared distance can be expressed as

$$d_i^2 = \left(\sqrt{\frac{\theta_0 + c_i^2\theta_1 + \theta_0\theta_1}{1+\theta_1}} - r_i \right)^2 \quad \text{..} \quad \text{(A-21)}$$

Because this solution is concave upward, it is not compatible with the (σ, τ) data over the full range of σ. Instead of using it, we propose a hyperbolic, three-parameter equation that is physically meaningful.

The parametric equation is

$$f(\hat{\sigma}_i, \hat{\tau}_i, \theta) = \theta_0 + \theta_1\hat{\sigma}_i + \theta_2\hat{\sigma}_i^2 - \hat{\tau}_i^2 = 0 \quad \text{..} \quad \text{(A-22)}$$

Then Eq. A-12 becomes

$$[2(\hat{\sigma}_i - c_i) + (\theta_1 + 2\theta_2\hat{\sigma}_i)]\hat{\tau}_i = 0 \dots \dots (A\text{-}23)$$

For the squared distance, we have three different solutions.

If $\hat{\tau}_i = 0$, there are two solutions of the squared distance, given by.

$$d_i^2 = \left(\sqrt{(\hat{\sigma}_i - c_i)^2} - r_i \right)^2 \dots \dots (A\text{-}24)$$

where

$$\hat{\sigma}_i = \frac{\theta_1 \pm \sqrt{\theta_1^2 - 4\theta_0\theta_2}}{2\theta_2} \dots \dots (A\text{-}25)$$

And the third solution of the squared distance is given by

$$d_i^2 = \left(\sqrt{(\hat{\sigma}_i - c_i)^2 + \theta_0 + \theta_1\hat{\sigma}_i + \theta_2\hat{\sigma}_i^2} - r_i \right)^2 \dots \dots (A\text{-}26)$$

where

$$\hat{\sigma}_i = \frac{c_i - \theta_1/2}{(1 + \theta_2)} \dots \dots (A\text{-}27)$$

Fitting failure envelope in the principal stress plane

From a triaxial test we can obtain the raw data, which neglect the principal intermediate stress and obtain a parametric representation of the envelope directly in the principal stress plane. The model could be written in its implicit form as Eq. A-28:

$$g(\hat{\sigma}_3, \hat{\sigma}_1, \underline{\theta}') = 0 , \dots \dots (A\text{-}28)$$

where

$\hat{\sigma}_3$ = corrected or "reconciled" lateral stress

$\hat{\sigma}_1$ = corrected or "reconciled" axial stress

$\underline{\theta'}$ = vector of unknown parameters

Our goal is to find the optimum parameters at which the sum of necessary corrections squared,

$$J = \sum_{i=1}^{n} d_{p_i}^2 \text{,} \dots\dots\dots\dots\dots\dots\dots\dots\dots\dots\dots\dots\dots\dots\dots\dots\dots \quad \text{(A-29)}$$

is minimum, where for each pair of measurements,

$$d_{p_i}^2 = \left(\hat{\sigma}_{3i} - \sigma_{3i}\right)^2 + \left(\hat{\sigma}_{1i} - \sigma_{1i}\right)^2 \dots\dots\dots\dots\dots\dots\dots\dots\dots\dots\dots\dots \quad \text{(A-30)}$$

Fig. A-3 shows the correction corresponds to the true distance of the point from the algebraic curve using EIV method (d_{pi}).

Error-in-variables algorithm applied to the principal stress plane

In **Fig. A-4** the measured points have been reconciled by using the EIV approach.
Let a, denote the tangent vector of the envelope at

$$a = -\frac{\partial g\left(\hat{\sigma}_{3i}\hat{\sigma}_{1i}, \theta'\right)}{\partial \hat{\sigma}_1} i + \frac{\partial g\left(\hat{\sigma}_{3i}\hat{\sigma}_{1i}, \theta'\right)}{\partial \hat{\sigma}_3} j \dots\dots\dots\dots\dots\dots\dots\dots\dots \quad \text{(A-31)}$$

and **b** the vector from the measured i-th point to the envelope:

$$b = \left(\hat{\sigma}_{3i} - \sigma_{3i}\right)i + \left(\hat{\sigma}_{1i} - \sigma_{1i}\right)j \dots\dots\dots\dots\dots\dots\dots\dots\dots\dots \quad \text{(A-32)}$$
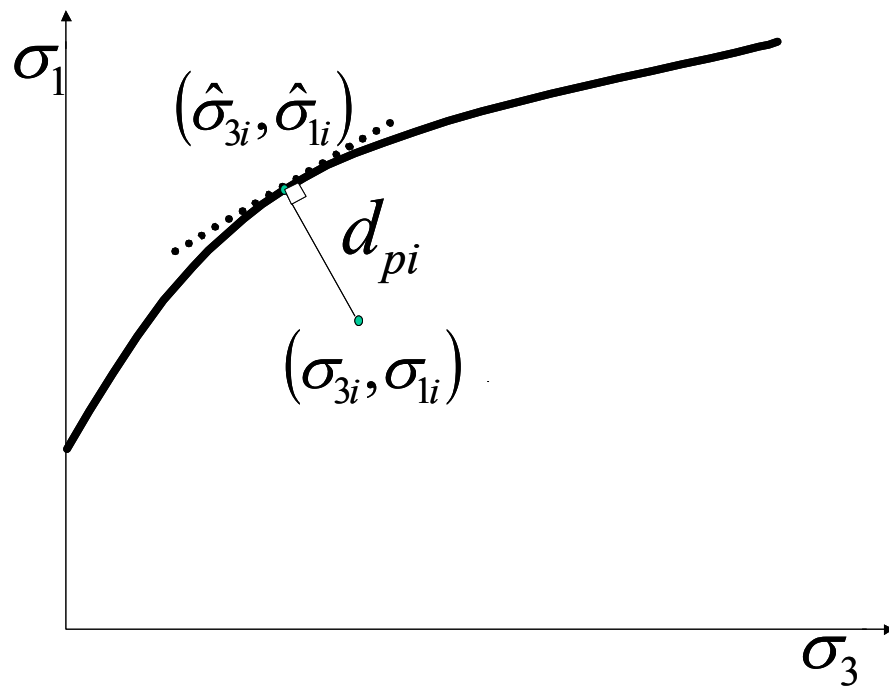
Fig. A-3- Geometric representation of the distance from EIV in the principal stress plane.
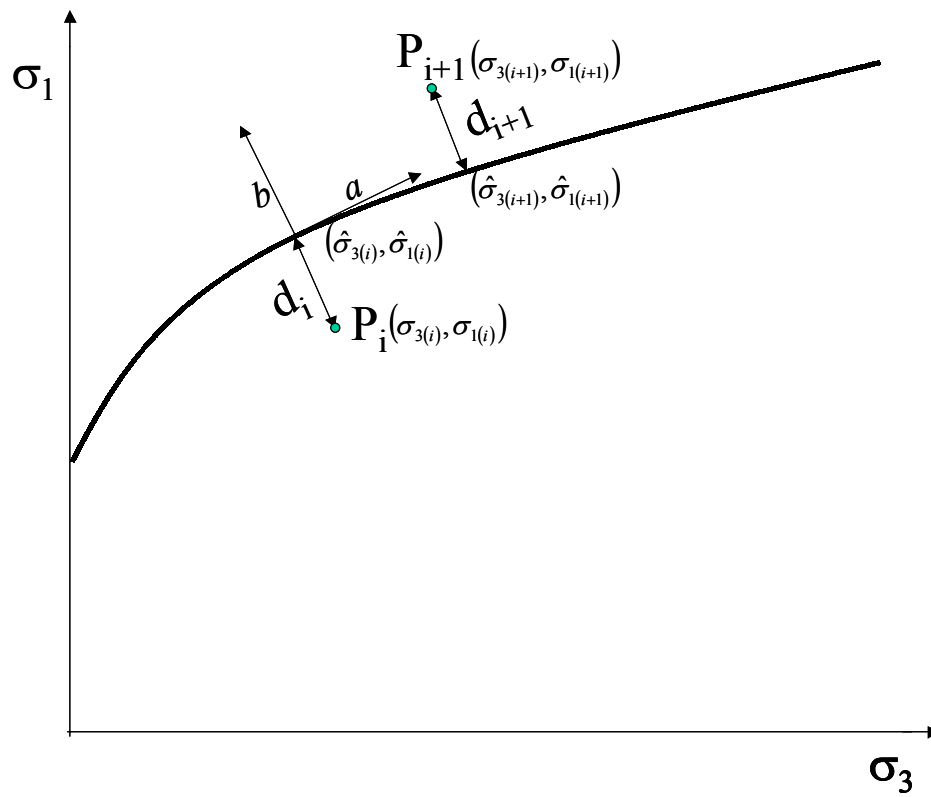
Fig.A-4- Graphic representation of the EIV algorithm in the principal stress plane.

From EIV, a and b must be orthogonal, $a \cdot b = 0$:

$$-\left(\hat{\sigma}_{3i} - \sigma_{3i}\right)\frac{\partial g\left(\hat{\sigma}_{3i}\hat{\sigma}_{1i},\underline{\theta}'\right)}{\partial \hat{\sigma}_1} + \left(\hat{\sigma}_{1i} - \sigma_{1i}\right)_i \frac{\partial g\left(\hat{\sigma}_{3i}\hat{\sigma}_{1i},\underline{\theta}'\right)}{\partial \hat{\sigma}_3} = 0 \quad \text{....................} \quad \text{(A-33)}$$

The system of Eqs. A-28 and A-33 can be solved simultaneously to obtain $\left(\hat{\sigma}_3, \hat{\sigma}_1\right)$ at any parameter vector $\underline{\theta}'$, evaluating the objective function.

Linear and parabolic function can be considered to represent the failure envelope at the principal stress plane. We may not need more complex function to fit the failure envelope in the principal stress plane.

Application to selected models

Linear envelope equation

Thus, Eq. A-28 can be expressed as

$$g\left(\hat{\sigma}_{3i}, \hat{\sigma}_{1i}, \underline{\theta}'\right) = \theta_0' + \theta_1' \hat{\sigma}_{3i} - \hat{\sigma}_{1i} = 0 , \quad \text{..................................} \quad \text{(A-34)}$$

where, θ_0' and θ'_1 are the parameters of the linear envelope. Eq. A-33 can be represented as

$$\left(\hat{\sigma}_{3i} - \sigma_{3i}\right) + \theta_1'\left(\hat{\sigma}_{1i} - \sigma_{1i}\right) = 0 \quad \text{..} \quad \text{(A-35)}$$

Solving the system of Eqs. A-34 and A-35, the solution for the squared distance can be represent by Eq. A-30, having

$$\hat{\sigma}_{3i} = -\frac{\theta_0'\theta_1' + \theta_1'\sigma_{1i} - \sigma_{3i}}{1 + \theta_1'^2} \quad \text{..} \quad \text{(A-36)}$$

and

$$\hat{\sigma}_{1i} = \frac{-\theta_0' - \theta_1'^2 \sigma_{1i} - \theta_1' \sigma_{3i}}{1 + \theta_1'^2} \quad\text{...(A-37)}$$

Substituting Eq. A-30 into the objective function Eq. A-28 we arrive at an unconstrained minimization problem involving two unknown parameters: θ_0' and θ_1'.

Parabolic envelope equation

For the parabolic approximation of the envelope, Eq. A-28 can be written as

$$g(\hat{\sigma}_{3i}, \hat{\sigma}_{1i}, \underline{\theta'}) = \theta_0' + \theta_1' \; \hat{\sigma}_{3i} - \hat{\sigma}_{1i}^2 = 0 \quad\text{..} \quad\text{(A-38)}$$

where θ_0' and θ_1' are the parameters. The appropriate form of Eq. A-33 is

$$\theta_1'(\hat{\sigma}_{1i} - \sigma_{1i}) - 2\hat{\sigma}_{1i}(\hat{\sigma}_{3i} - \sigma_{3i}) = 0 \quad\text{..} \quad\text{(A-39)}$$

Solving the system of Eqs. A-38 and A-39 we obtain the squared distance by Eq. A-30. Because of the cumbersome nature of the $\hat{\sigma}_{3i}$ roots, the squared distance, d_i^2, is not shown for the parabolic envelope.

Fitting failure envelope including poroelastic effect

The group of parametric equations of the failure envelope developed in the principal-stress plane can be modified in a very simple way by introducing the concept of poroelasticity of Biot. The state of stress can be represented by the equivalent stress (σ_{eq}) and the effective mean stress (σ_m') as stress invariants that are independent of coordinate rotation. This two invariant can be written as:

$$\sigma'_m = (\sigma_1 + 2\sigma_3)/3 - \alpha p_p \dots\dots\dots\dots\dots\dots\dots\dots\dots\dots\dots\dots\dots\dots \quad \text{(A-40)}$$

and

$$\sigma_{eq} = \sqrt{3J_2} = \sigma_1 - \sigma_3, \dots\dots\dots\dots\dots\dots\dots\dots\dots\dots\dots\dots\dots \quad \text{(A-41)}$$

where p_p is reservoir pore pressure, and $\alpha = 1 - \dfrac{c_{ma}}{c_b}$ (c_{ma} is the matrix compressibility; c_b is the bulk compressibility).

For porous sandstones: $c_{ma} \ll c_b$, so $\alpha \rightarrow 1$.

Eqs. A-40 and A-41 represent the mean effective stress and the equivalent stress respectively, and J_2 is the second invariant of the stress deviator tensor.

Using those equations and the EIV approach, we can generate an algebraic solution for the material that will satisfy the equation of the envelope given in implicit form as

$$h(\hat{\sigma}_m, \hat{\sigma}_{eq}, \underline{\theta''}) = 0 \dots\dots\dots\dots\dots\dots\dots\dots\dots\dots\dots\dots\dots\dots\dots \quad \text{(A-42)}$$

A similar procedure to the EIV approach used in the (σ_3, σ_1) stress plane could be applied.

Our goal is to find the optimum parameters at which the sum of necessary corrections squared. We can express Eq A-30 in terms of the mean effective stress and the equivalent stress as follow,

$$d_{p_i}^2 = (\hat{\sigma}'_{mi} - \sigma'_{mi})^2 + (\hat{\sigma}_{eqi} - \sigma_{eqi})^2 \dots\dots\dots\dots\dots\dots\dots\dots\dots\dots\dots \quad \text{(A-43)}$$

Because the failure envelope is fitting in the principal effective stress plane, we can apply the EIV algorithm used for the principals stress plane applied and can be simplify

Error-in-variables algorithm applied to the principal effective stress plane

Then vector a, given by Eq. A-31 can be expressed as

$$a = -\frac{\partial h(\hat{\sigma}'_{mi}, \hat{\sigma}_{eqi}, \underline{\theta}'')}{\partial \hat{\sigma}_{eq}} i + \frac{\partial h(\hat{\sigma}'_{mi}, \hat{\sigma}_{eqi}, \underline{\theta}'')}{\partial \hat{\sigma}'_{m}} j \quad \text{(A-44)}$$

while vector b, given by Eq. A-32 is expressed as

$$b = (\hat{\sigma}'_{mi} - \sigma'_{mi})i + (\hat{\sigma}_{eqi} - \sigma_{eqi})j \quad \text{(A-45)}$$

Eq. A-33 which represent the orthogonality between vector a and b is expressed as

$$-(\hat{\sigma}'_{mi} - \sigma'_{mi})\frac{\partial h(\hat{\sigma}'_{mi}\hat{\sigma}_{eqi}, \underline{\theta}'')}{\partial \hat{\sigma}_{eq}} + (\hat{\sigma}_{eqi} - \sigma_{eqi})_i \frac{\partial h(\hat{\sigma}'_{mi}\hat{\sigma}_{eqi}, \underline{\theta}'')}{\partial \hat{\sigma}'_{m}} = 0 \quad \text{(A-46)}$$

The system of Eqs. A-42 and A-46 can be solved simultaneously to obtain $(\hat{\sigma}'_m, \hat{\sigma}_{eq})$ at any parameter vector $\underline{\theta}''$, evaluating the objective function.

In addition to the linear and parabolic function considered representing the failure envelope at the principal-stress plane, we propose three parameter equations to fit the failure envelope when including poroelastic effect.

Selected models

In this case both the linear and parabolic envelope equations can be used introducing the mean-effective-stress and the equivalent-stress definitions, so that Eqs. A-34 through A-

37 can be expressed in terms of $\left(\hat{\sigma}'_m, \hat{\sigma}_{eq}\right)$ for the linear envelope and Eqs. A-38 and A-39 for the parabolic envelope.

Hence, for the linear envelope Eq. A-34 becomes

$$h\left(\hat{\sigma}'_{mi}, \hat{\sigma}_{eqi}, \underline{\theta''}\right) = \theta''_0 + \theta''_1 \; \hat{\sigma}'_{mi} - \hat{\sigma}_{eqi} = 0, \dots\dots\dots\dots\dots\dots\dots\dots\dots\dots\dots \text{(A-47)}$$

while eq.(A-35) can be represented as

$$\left(\hat{\sigma}'_{mi} - \sigma'_{mi}\right) + \theta''_1\left(\hat{\sigma}_{eqi} - \sigma_{eqi}\right) = 0 \dots\dots\dots\dots\dots\dots\dots\dots\dots\dots \text{(A-48)}$$

Solving the system of Eqs. A-47 and A-48 the solution for the squared distance can be represented by Eq. A-43,
where,

$$\hat{\sigma}'_{mi} = -\frac{\theta''_0\theta''_1 + \theta''_1\sigma_{eqi} - \sigma'_{mi}}{1 + \theta''^2_1} \dots\dots\dots\dots\dots\dots\dots\dots\dots\dots\dots \text{(A-49)}$$

and

$$\hat{\sigma}_{eqi} = \frac{-\theta''_0 - \theta''^2_1\sigma_{eqi} - \theta''_1\sigma'_{mi}}{1 + \theta''^2_1} \dots\dots\dots\dots\dots\dots\dots\dots\dots\dots \text{(A-50)}$$

For the parabolic approximation of the envelope, Eq. A-38 can be written as

$$h\left(\hat{\sigma}'_{mi}, \hat{\sigma}_{eqi}, \underline{\theta''}\right) = \theta''_0 + \theta''_1 \; \hat{\sigma}'_{mi} - \hat{\sigma}^2_{eqi} = 0 \dots\dots\dots\dots\dots\dots\dots\dots\dots \text{(A-51)}$$

and Eq. A-39 can be expressed as

$$\theta''_1\left(\hat{\sigma}_{eqi} - \sigma_{eqi}\right) - 2\hat{\sigma}_{1i}\left(\hat{\sigma}'_{mi} - \sigma'_{mi}\right) = 0 \dots\dots\dots\dots\dots\dots\dots\dots\dots \text{(A-52)}$$

Solving the system of Eqs. A-51 and A-52 we obtain the squared distance from Eq. A-43.

We propose three-parameter equations to fit the failure envelope in the principal effective-stress plane if only brittle behavior is considered. Then, Eq. A-42 can be written either as

$$h\left(\hat{\sigma}'_{mi}, \hat{\sigma}_{eqi}, \underline{\theta''}\right) = \theta''_0 + \theta''_1 \hat{\sigma}'_{mi} + \theta''_2 \hat{\sigma}'^2_{mi} - \hat{\sigma}^2_{eqi} = 0 \dots\dots\dots\dots\dots\dots\dots\dots\text{(A-53)}$$

while Eq. A-46 become

$$\left(\theta''_1 + 2\theta''_2 \hat{\sigma}'_{mi}\right)\left(\hat{\sigma}_{eqi} - \sigma_{eqi}\right) - 2\hat{\sigma}_{eqi}\left(\sigma'_{mi} - \hat{\sigma}'_{mi}\right) = 0 \dots\dots\dots\dots\dots\dots\text{(A-54)}$$

or

$$h\left(\hat{\sigma}'_{mi}, \hat{\sigma}_{eqi}, \underline{\theta''}\right) = \theta''_0 + \theta''_1 \hat{\sigma}'_{mi} - \theta''_2 \hat{\sigma}_{eqi} - \hat{\sigma}^2_{eqi} = 0 \dots\dots\dots\dots\dots\dots\text{(A-55)}$$

$$\left(\theta''_1\right)\left(\hat{\sigma}_{eqi} - \sigma_{eqi}\right) - \left(2\hat{\sigma}_{eqi} + \theta''_2\right)\left(\hat{\sigma}'_{mi} - \sigma'_{mi}\right) = 0 \dots\dots\dots\dots\dots\dots\text{(A-56)}$$

Solving either the system of Eqs. A-53 and A-54, or A-55 and A-56, we obtain the squared distance by Eq. A-43.

Applying the method to special models suitable for describing brittle-ductile transition in yield envelope

Using the concept of invariants or effective-stresses state in the plane, we can obtain the failure or yield envelope when considering pore collapse.

Using the EIV approach, we can generate an algebraic solution for the brittle-to-ductile transition behavior of the material, considering pore collapse that will satisfy the equation of the envelope given in implicit form as

$$h\left(\hat{\sigma}_m, \hat{\sigma}_{eq}, \underline{\theta''}\right) = 0 \dots\dots\dots\dots\dots\dots\dots\dots\dots\dots\dots\dots\dots\dots\dots\dots\text{(A-57)}$$

The parametric representation proposed to fit the failure envelope in the principal effective stress plane when considering pore collapse is given by a four parameters equation that can fit the envelope in such a way that cover from the brittle region passing through the transitional region until reach the ductile region defining the pore collapse as a cap model. Then, Eq. A-42 can be written as

$$h\left(\hat{\sigma}'_{mi}, \hat{\sigma}_{eqi}, \underline{\theta''}\right) = \theta''_0 + \theta''_1 \hat{\sigma}'_{mi} + \theta''_2 \hat{\sigma}'^2_{mi} - \theta''_3 \hat{\sigma}_{eqi} - \hat{\sigma}^2_{eqi} = 0 \dots\dots\dots\dots\text{(A-58)}$$

while Eq. A-46 become

$$\left(\theta''_1 + 2\theta''_2 \hat{\sigma}'_{mi}\right)\left(\hat{\sigma}_{eqi} - \sigma_{eqi}\right) - \left(\theta''_3 + 2\hat{\sigma}_{eqi}\right)\left(\sigma'_{mi} - \hat{\sigma}'_{mi}\right) = 0 \dots\dots\dots\dots\dots\text{(A-59)}$$

Solving the system of Eqs. A-58 and A-59 we obtain the squared distance from Eq. A-43.

Generalizing Balmer's method to obtain a parametric representation in Mohr's plane from the representation in the principal stress plane

Using the resulting EIV parametric representation of the failure envelope in the principal stress plane Eq. A-28 we can transform the algebraic solution to a parametric representation in the Mohr plane. Balmer[10] suggested an analytical relationship between (σ, τ) and the principal-stress components for the Mohr failure criterion. Recall that the normal and shear stress at failure is represent in the Mohr plane as

$$\sigma = \left(\frac{\sigma_1 + \sigma_3}{2}\right) + \left(\frac{\sigma_1 - \sigma_3}{2}\right) Cos(2\alpha) \qquad \text{(A-60)}$$

$$\tau = \left(\frac{\sigma_1 - \sigma_3}{2}\right) Sin(2\alpha) \qquad \text{(A-61)}$$

Then the reconciled values obtained from the EIV method in the principal-stress plane are introduced in Balmer's solution for the Mohr failure criterion. Balmer's equations, which were derived from Eq. A-1 can be expressed in terms of the reconciled values of $(\hat{\sigma}_3, \hat{\sigma}_1)$:

$$\hat{\sigma} = \hat{\sigma}_3 + \frac{\hat{\sigma}_1 - \hat{\sigma}_3}{\dfrac{d\hat{\sigma}_1}{d\hat{\sigma}_3} + 1}, \dotfill \text{(A-62)}$$

$$\hat{\tau} = \frac{\hat{\sigma}_1 - \hat{\sigma}_3}{\dfrac{d\hat{\sigma}_1}{d\hat{\sigma}_3} + 1} \sqrt{\dfrac{d\hat{\sigma}_1}{d\hat{\sigma}_3}} \quad \text{...} \quad \text{(A-63)}$$

If we consider picking up two consecutive points of the resulting failure envelope in the principal stress plane (as shown in Fig. A-5), we can map out the constitutive equation of the envelope in the Mohr plane. That is, if we denote,

$$\hat{\sigma}_3^{(i)} = \hat{\sigma}_3, \text{...} \quad \text{(A-64)}$$

$$\hat{\sigma}_3^{(i+1)} = \hat{\sigma}_3 + d\hat{\sigma}_3, \text{...} \quad \text{(A-65)}$$

$$\hat{\sigma}_1^{(i)} = \hat{\sigma}_1, \text{...} \quad \text{(A-66)}$$

$$\hat{\sigma}_1^{(i+1)} = \hat{\sigma}_1 + \left(\dfrac{d\hat{\sigma}_1}{d\hat{\sigma}_3} \right) d\hat{\sigma}_3, \text{...} \quad \text{(A-67)}$$

Then we can expressed Eqs. A-62 and A-63 as

$$\hat{\sigma}^{(i)} = \hat{\sigma}_3^{(i)} + \frac{\hat{\sigma}_1^{(i)} - \hat{\sigma}_3^{(i)}}{\dfrac{d\hat{\sigma}_1}{d\hat{\sigma}_3} + 1}, \text{...} \quad \text{(A-68)}$$

and

$$\hat{\tau}^{(i)} = \frac{\hat{\sigma}_1^{(i)} - \hat{\sigma}_3^{(i)}}{\dfrac{d\hat{\sigma}_1}{d\hat{\sigma}_3} + 1} \sqrt{\dfrac{d\hat{\sigma}_1}{d\hat{\sigma}_3}} \quad \text{...} \quad \text{(A-69)}$$

and

$$\hat{\sigma}^{(i+1)} = \hat{\sigma}_3^{(i+1)} + \frac{\hat{\sigma}_1^{(i+1)} - \hat{\sigma}_3^{(i+1)}}{\dfrac{d\hat{\sigma}_1}{d\hat{\sigma}_3} + 1}, \dotfill \text{(A-70)}$$

$$\hat{\tau}^{(i)} = \frac{\hat{\sigma}_1^{(i)} - \hat{\sigma}_3^{(i)}}{\dfrac{d\hat{\sigma}_1}{d\hat{\sigma}_3} + 1} \sqrt{\frac{d\hat{\sigma}_1}{d\hat{\sigma}_3}} \dotfill \text{(A-71)}$$

Subtracting Eq. A-70 from Eq. A-68 and Eq. A-71 from Eq. A-69 and introducing Eqs. A-64 through A-67, we obtained

$$\frac{\hat{\sigma}^{(i+1)} - \hat{\sigma}^{(i)}}{d\hat{\sigma}_3} = \frac{2\dfrac{d\hat{\sigma}_1}{d\hat{\sigma}_3}}{\dfrac{d\hat{\sigma}_1}{d\hat{\sigma}_3} + 1}, \dotfill \text{(A-72)}$$

$$\frac{\hat{\tau}^{(i+1)} - \hat{\tau}^{(i)}}{d\hat{\sigma}_3} = \frac{\dfrac{d\hat{\sigma}_1}{d\hat{\sigma}_3} - 1}{\dfrac{d\hat{\sigma}_1}{d\hat{\sigma}_3} + 1} \sqrt{\frac{d\hat{\sigma}_1}{d\hat{\sigma}_3}} \dotfill \text{(A-73)}$$

Dividing Eq. A-72 by Eq. A-73, we obtain

$$\frac{d\hat{\tau}}{d\hat{\sigma}} = \frac{\dfrac{d\hat{\sigma}_1}{d\hat{\sigma}_3} - 1}{2\sqrt{\dfrac{d\hat{\sigma}_1}{d\hat{\sigma}_3}}}, \dotfill \text{(A-74)}$$

where

$$\frac{d\hat{\sigma}_1}{d\hat{\sigma}_3} = \frac{dg(\hat{\sigma}_3, \hat{\sigma}_1, \underline{\theta}')}{d\hat{\sigma}_3} \dotfill \text{(A-75)}$$

Solving simultaneously Eqs. A-28, A-62 and A-63, considering Eq. A-75, and recalling that from EIV we must preserve the orthogonallity, we obtain a parametric solution in (σ,τ) stress plane. The expression for the failure envelope in the Mohr plane is given by

$$f(\hat{\sigma},\hat{\tau},\underline{\theta'})=0 \dots\dots\dots\dots\dots\dots\dots\dots\dots\dots\dots\dots\dots\dots\dots\dots\dots\dots\dots\text{(A-76)}$$

It is important to notice that a closed-form solution may or may not be achieved analytically; however, we can also treat a numerical approximation.

To illustrate the transformation of the failure envelope from the principal-stress plane to the Mohr plane, we present the parametric representation of the linear and parabolic models obtained in the principal-stress plane in the Mohr plane.

Transformation of select models

We can use the resulting EIV parametric representation of the failure envelope in the principal stress plane Eq. A-34 for the linear model. To transform into the Mohr plane we derive Eq. A-34 to equation A-75 :

$$\frac{d\hat{\sigma}_1}{d\hat{\sigma}_3}=\frac{dg(\hat{\sigma}_{3i},\hat{\sigma}_{1i},\theta')}{d\hat{\sigma}_3}=\theta'_1 \qquad\qquad\qquad\text{(A-77)}$$

Then Eqs. A-62 and A-63 can be expressed as

$$\hat{\sigma}_i=\hat{\sigma}_{3i}+\frac{\hat{\sigma}_{1i}-\hat{\sigma}_{3i}}{\theta'_1+1} \qquad\qquad\qquad\text{(A-78)}$$

and

$$\hat{\tau}_i = \frac{\hat{\sigma}_{1i} - \hat{\sigma}_{3i}}{\theta_1' + 1}\sqrt{\theta_1'} \qquad (A\text{-}79)$$

Solving simultaneously Eqs. A-34, A-78 and A-79 the resulting parametric solution in the (σ, τ) stress plane is expressed as

$$f(\hat{\sigma}_i, \hat{\tau}_i, \theta') = \frac{\sqrt{\hat{\sigma}_i^{\,2} - 2\hat{\sigma}_i\theta_0' + \theta_0'^2 - 2\hat{\sigma}_i^{\,2}\theta_1' + 2\hat{\sigma}_i\theta_0'\theta_1' + \hat{\sigma}_i^{\,2}\theta_1'^2}}{\sqrt{\theta_1'}} - \hat{\tau}_i \qquad (A\text{-}80)$$

This demands that $\theta_1' \geq 0$ exist.

For the parabolic model Eq. A-38 can be transformed into a parametric representation in the Mohr plane. Let us assume that we have obtained the EIV parametric representation of the failure envelope in the principal-stress plane. That is, we have determined the optimum parameters of the parabolic model, Eq. A-38. To transform into the Mohr plane, we derive Eq. A-38 to Eq. A-75 as

$$\frac{d\hat{\sigma}_1}{d\hat{\sigma}_3} = \frac{dg(\hat{\sigma}_{3i}, \hat{\sigma}_{1i}, \theta')}{d\hat{\sigma}_3} = \frac{\theta_1'}{2\sqrt{\theta_0' + \theta_1'\hat{\sigma}_{3i}}} \qquad (A\text{-}81)$$

In this case, Eqs. A-62 and A-63 can be expressed as

$$\hat{\sigma}_i = \hat{\sigma}_{3i} + \frac{\hat{\sigma}_{1i} - \hat{\sigma}_{3i}}{\dfrac{\theta_1'}{2\sqrt{\theta_0' + \theta_1'\hat{\sigma}_{3i}}} + 1} \qquad (A\text{-}82)$$

and

$$\hat{\tau}_i = \frac{\hat{\sigma}_{1i} - \hat{\sigma}_{3i}}{\dfrac{\theta_1'}{2\sqrt{\theta_0' + \theta_1'\hat{\sigma}_{3i}}} + 1} \sqrt{\frac{\theta_1'}{2\sqrt{\theta_0' + \theta_1'\hat{\sigma}_{3i}}}} \quad \dots\dots\dots\dots\dots\dots\dots\dots\dots\dots\dots\dots\dots\dots \quad \text{(A-83)}$$

Solving simultaneously Eqs. A-38, A-82 and A-83, the resulting parametric solution in the (σ, τ) stress plane is expressed as

$$f(\hat{\sigma}_i, \hat{\tau}_i, \theta') = -\frac{2\hat{\sigma}_i^{\,2}}{3} + \frac{2\hat{\sigma}_i}{27\theta_1'} - \frac{2\hat{\sigma}_i\theta_0'}{3\theta_1'} + \frac{2\left(\sigma_i^{\,2} + 3\theta_0' + 3\sigma_i\theta_1'\right)^{3/2}}{27\theta_1'} - \tau_i^2 \quad \dots\dots \quad \text{(A-84)}$$

Since the slope $\dfrac{d\hat{\sigma}_1}{d\hat{\sigma}_3}$ given by Eq. A-81 must exist, the square-root term must be greater than or equal to zero. In addition, because the slope depends on σ_3, it should increase when the values of such variable increase; thus, the slope must be positive. This implies that such generated envelope can describe the failure criteria for the brittle region of the tested rock.

We assumed that the quantity under the square root is always positive; that is automatically satisfied, for example, in the brittle region.
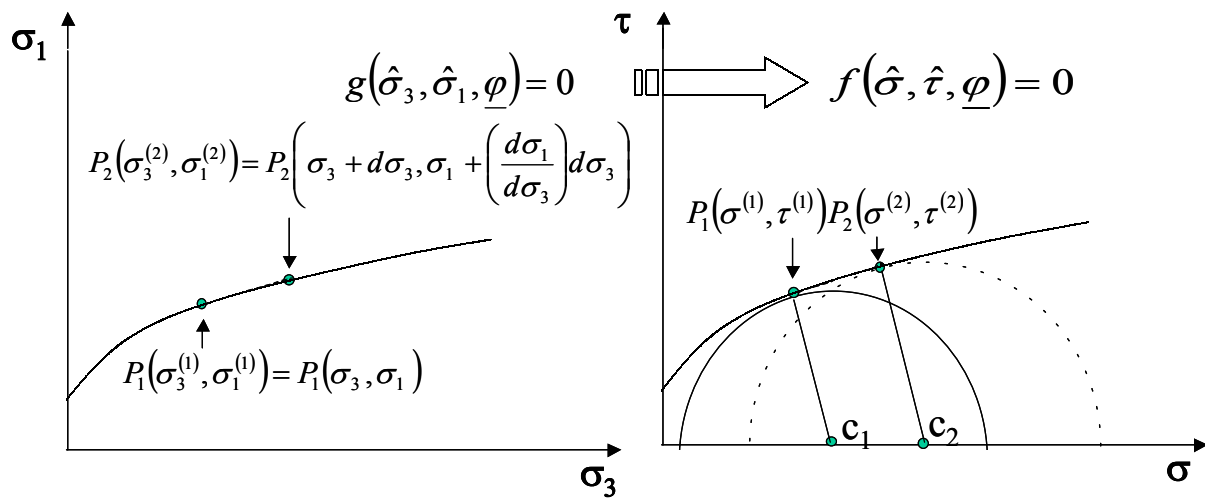
Fig. A-5- Graphic representation of the failure envelope's transformation from the principal stress plane to the Mohr plane using EIV method.

APPENDIX B

DERIVATION OF THE PARAMETRIC REPRESENTATION FOR FAILURE CRITERIA IN 3D

Introduction

The objective of this appendix is to present the methodology to obtain the parametric representation of the failure surface using the error-in-variables (EIV) method. The mathematical derivations to fit the failure surface in the principal-stress space are presented in this appendix.

Fitting failure surface directly in the principal stress space

Typically, a failure criterion is expressed in terms of the major σ_1 and minor σ_3 principal stresses, neglecting or ignoring the influence of the principal intermediate stress σ_2; but in some case the influence of the principal intermediate cannot be disregard. For this reason, a three-dimensional failure criterion is required. A delimiting failure surface can be represented by:

$$g(\sigma_1, \sigma_2, \sigma_3) = 0 \dots\dots\dots\dots\dots\dots\dots\dots\dots\dots\dots\dots\dots\dots\dots\dots\dots\dots\dots (B-1)$$

Under the principal-stress coordinate, there are only three nonzero stress $(\sigma_1, \sigma_2, \sigma_3)$ components. To obtain the delimiting surface, we need a method of data fitting. In our research, the parametric representation of the failure surface can be obtained through the statistics-based method of error-in-variables that considers all the measured variables

having experimental error. Here we present the application of this methodology to fit the failure surface.

Application of EIV method to fit failure surface

In 3D the model could be written in its implicit form as Eq. B-2,

$$g(\hat{\sigma}_1, \hat{\sigma}_2, \hat{\sigma}_3, \underline{\theta}') = 0, \dotfill \text{(B-2)}$$

where

$\hat{\sigma}_3$ = corrected or "reconciled" minimum principal stress
$\hat{\sigma}_2$ = corrected or "reconciled" intermediate principal stress
$\hat{\sigma}_1$ = corrected or "reconciled" maximum principal stress
$\underline{\theta}'$ = vector of unknown parameters

We are looking for the optimum parameters that minimize the sum of the squared distance,

$$J = \sum_{i=1}^{n} d_{p_i}^2, \dotfill \text{(B-3)}$$

which for each pair of measurements is given by

$$d_{p_i}^2 = \left(\hat{\sigma}_{1i} - \sigma_{1i}\right)^2 + \left(\hat{\sigma}_{2i} - \sigma_{2i}\right)^2 + \left(\hat{\sigma}_{3i} - \sigma_{3i}\right)^2 \dotfill \text{(B-4)}$$

The measured variables are given by $(\sigma_1, \sigma_2, \sigma_3)$.

Since a surface represents the limit between stable and unstable zones of stress state in the space, we defined algorithm in terms of the perpendicular line to the surface and the measured points using the concept of error-in-variables, which considers the shortest distance to reconcile each point to the surface.

For a general function given by Eq. B-1, the perpendicular line to the surface is represented by the gradients.

$$\left(\frac{\partial g(\sigma_1,\sigma_2,\sigma_3)}{\partial \sigma_1}, \frac{\partial g(\sigma_1,\sigma_2,\sigma_3)}{\partial \sigma_2}, \frac{\partial g(\sigma_1,\sigma_2,\sigma_3)}{\partial \sigma_3} \right) \dots\dots\dots\dots\dots\dots\dots\dots\dots\dots \quad \text{(B-5)}$$

Error-in-variables algorithm applied to the principal stress space

Eq. B-1 can be expressed in a general form:

$$g(\sigma_1',\sigma_2',\sigma_3',\underline{\theta'}) = 0 \dots\dots\dots\dots\dots\dots\dots\dots\dots\dots\dots\dots\dots\dots\dots\dots \quad \text{(B-6)}$$

Then to reconcile the measurements to the general surface, we must find the shortest distance to the surface as follow:

$$\left(\frac{\partial g(\sigma_1',\sigma_2',\sigma_3',\underline{\theta'})}{\partial \sigma_1} \right) = k(\hat{\sigma}_1 - \sigma_1) \dots\dots\dots\dots\dots\dots\dots\dots\dots\dots\dots\dots \quad \text{(B-7)}$$

$$\left(\frac{\partial g(\sigma_1',\sigma_2',\sigma_3',\underline{\theta'})}{\partial \sigma_2} \right) = k(\hat{\sigma}_2 - \sigma_2) \dots\dots\dots\dots\dots\dots\dots\dots\dots\dots\dots\dots \quad \text{(B-8)}$$

$$\left(\frac{\partial g(\sigma_1',\sigma_2',\sigma_3',\underline{\theta'})}{\partial \sigma_3} \right) = k(\hat{\sigma}_3 - \sigma_3) \dots\dots\dots\dots\dots\dots\dots\dots\dots\dots\dots\dots \quad \text{(B-9)}$$

where

$(\sigma_1, \sigma_2, \sigma_3)$ are the measured variables

$(\hat{\sigma}_1, \hat{\sigma}_2, \hat{\sigma}_3)$ are the reconciled variables

$(\sigma'_1, \sigma'_2, \sigma'_3)$ are the general variables

k is the proportional distance from the measured points to the surface.

To validate the proposed methodology we consider the algebraic form of the equations for the elliptic cone and elliptic paraboloid. Next we stated the constitutive equation that represents the two proposed 3D models.

Application to selected models

Elliptic cone surface equation

Thus, equation (B-2) can be expressed as

$$g\left(\sigma'_{1i}, \sigma'_{2i}, \sigma'_{3i}, \underline{\theta'}\right) = \theta'^2_1 \sigma'^2_{3i} + \theta'^2_2 \sigma'^2_{2i} - \theta'^2_3 \sigma'^2_{1i} = 0 \quad\ldots\ldots\ldots\ldots\ldots\ldots\ldots\ldots\ldots \quad \text{(B-10)}$$

where, θ'_1, θ'_2 and θ'_3 are the parameters of the elliptic cone surface. Eq. (B-7), (B-8) and (B-9) can be represented as.

$$\left(-2\theta'_3 \sigma'_{1i}\right) = k\left(\hat{\sigma}_{1i} - \sigma_{1i}\right) \quad\ldots\ldots\ldots\ldots\ldots\ldots\ldots\ldots\ldots\ldots\ldots\ldots \quad \text{(B-11)}$$

$$\left(2\theta'_2 \sigma'_{2i}\right) = k\left(\hat{\sigma}_{2i} - \sigma_{2i}\right) \quad\ldots\ldots\ldots\ldots\ldots\ldots\ldots\ldots\ldots\ldots\ldots\ldots\ldots\ldots \quad \text{(B-12)}$$

$$\left(2\theta'_1 \sigma'_{3i}\right) = k\left(\hat{\sigma}_{3i} - \sigma_{3i}\right) \quad\ldots\ldots\ldots\ldots\ldots\ldots\ldots\ldots\ldots\ldots\ldots\ldots\ldots \quad \text{(B-13)}$$

Solving the system of equations (B-10) through (B-13) and recalling that we must reconciled the measured points at the general surface obtaining the following solutions for $\hat{\sigma}_{3i}$.

$$\hat{\sigma}_{3i} = \frac{\theta'^2_3 \sigma_{3i} + \theta'_1 \theta'_3 \sigma_{1i}}{\theta'^2_1 + \theta'^2_3} \quad\ldots\ldots\ldots\ldots\ldots\ldots\ldots\ldots\ldots\ldots\ldots\ldots\ldots \quad \text{(B-14)}$$

and

$$\hat{\sigma}_{3i} = \frac{\theta_2' \theta_3' \sigma_{3i} \left(\theta_2' \sigma_{1i} + \theta_3' \sigma_{2i}\right)}{\theta_2' \sigma_{2i} \left(\theta_1'^2 + \theta_3'^2\right) + \theta_3' \sigma_{1i} \left(\theta_2'^2 - \theta_1'^2\right)} \quad\text{...}\text{(B-15)}$$

While for $\hat{\sigma}_{2i}$ we obtained the following solutions.

$$\hat{\sigma}_{2i} = \frac{\theta_3'^2 \sigma_{2i} + \theta_2' \theta_3' \sigma_{1i}}{\theta_2'^2 + \theta_3'^2} \quad\text{...}\text{(B-16)}$$

and

$$\hat{\sigma}_{2i} = \frac{\theta_1' \theta_3' \sigma_{2i} \left(\theta_1' \sigma_{1i} + \theta_3' \sigma_{3i}\right)}{\theta_1' \sigma_{3i} \left(\theta_2'^2 + \theta_3'^2\right) + \theta_3' \sigma_{1i} \left(\theta_1'^2 - \theta_2'^2\right)} \quad\text{...}\text{(B-17)}$$

Finally we can express equation B-10 as:

$$g\left(\hat{\sigma}_{1i}, \hat{\sigma}_{2i}, \hat{\sigma}_{3i}, \underline{\theta'}\right) = \theta_1'^2 \hat{\sigma}_{3i}^2 + \theta_2'^2 \hat{\sigma}_{2i}^2 - \theta_3'^2 \hat{\sigma}_{1i}^2 = 0 \quad\text{................................}\text{(B-18)}$$

Elliptic paraboloid surface equation

Thus, equation (B-2) can be expressed as

$$g\left(\sigma_{1i}', \sigma_{2i}', \sigma_{3i}', \underline{\theta'}\right) = \theta_1'^2 \sigma_{3i}'^2 + \theta_2'^2 \sigma_{2i}'^2 - \theta_3' \, \sigma_{1i}' = 0 \quad\text{.............................}\text{(B-19)}$$

where, θ_1', θ_2' and θ_3' are the parameters of the elliptic paraboloid surface. Eq. (B-7), (B-8) and (B-9) can be represented as.

$$\left(-\theta_3'\right) = k\left(\hat{\sigma}_{1i} - \sigma_{1i}\right) \quad\text{...}\text{(B-20)}$$

$$\left(2\theta_2'\sigma_{2i}'\right) = k\left(\hat{\sigma}_{2i} - \sigma_{2i}\right) \dotfill \text{(B-21)}$$

$$\left(2\theta_1'\sigma_{3i}'\right) = k\left(\hat{\sigma}_{3i} - \sigma_{3i}\right) \dotfill \text{(B-22)}$$

Solving the system of Eqs. B-19 through B-22 and recalling that we must reconcile the measured points at the general surface, we obtain the following solutions for $\hat{\sigma}_{3i}$:

$$\hat{\sigma}_{3i} = -\frac{\theta_3'\left(\theta_3' - 2\theta_1'^2\sigma_{1i}\right)}{y^{\frac{1}{3}}} + \frac{y^{\frac{1}{3}}}{6\theta_1'^4} \dotfill \text{(B-23)}$$

and

$$\hat{\sigma}_{3i} = \frac{\left(1 + i\sqrt{3}\right)\theta_3'\left(\theta_3' - 2\theta_1'^2\sigma_{1i}\right)}{2^{\frac{2}{3}}\left(2y\right)^{\frac{1}{3}}} + \frac{i\left(1 + \sqrt{3}\right)y^{\frac{1}{3}}}{12\theta_1'^4} \dotfill \text{(B-24)}$$

and

$$\hat{\sigma}_{3i} = \frac{\left(1 - i\sqrt{3}\right)\theta_3'\left(\theta_3' - 2\theta_1'^2\sigma_{1i}\right)}{2^{\frac{2}{3}}\left(2y\right)^{\frac{1}{3}}} - \frac{\left(1 + i\sqrt{3}\right)y^{\frac{1}{3}}}{12\theta_1'^4}, \dotfill \text{(B-25)}$$

where

$$y = 54\theta_1'^8\theta_3'^2\sigma_{3i} + \frac{\sqrt{x}}{2} \dotfill \text{(B-26)}$$

and

$$x = 11664\theta_1'^{16}\theta_3'^4\sigma_{3i}^2 + 864\theta_1'^{12}\theta_3'^3\left(\theta_3' - 2\theta_1'^2\sigma_{3i}^2\right)^3 \ldots\ldots\ldots\ldots\ldots\ldots\ldots\ldots\ldots \text{(B-27)}$$

In addition, if the imaginary part of those roots solutions is lower than or equal to 0.0001, the real part of the root is considered to be a solution.

For $\hat{\sigma}_{2i}$, we obtained the following solutions:

$$\hat{\sigma}_{2i} = -\frac{\theta_3'\left(\theta_3' - 2\theta_2'^2\sigma_{1i}\right)}{y^{1/3}} + \frac{y^{1/3}}{6\theta_2'^4} \ldots\ldots\ldots\ldots\ldots\ldots\ldots\ldots\ldots\ldots \text{(B-28)}$$

and

$$\hat{\sigma}_{3i} = \frac{\left(1 + i\sqrt{3}\right)\theta_3'\left(\theta_3' - 2\theta_2'^2\sigma_{1i}\right)}{2^{2/3}\left(2y\right)^{1/3}} + \frac{i\left(1 + \sqrt{3}\right)y^{1/3}}{12\theta_2'^4} \ldots\ldots\ldots\ldots\ldots\ldots \text{(B-29)}$$

and

$$\hat{\sigma}_{3i} = \frac{\left(1 - i\sqrt{3}\right)\theta_3'\left(\theta_3' - 2\theta_2'^2\sigma_{1i}\right)}{2^{2/3}\left(2y\right)^{1/3}} - \frac{\left(1 + i\sqrt{3}\right)y^{1/3}}{12\theta_2'^4} \ldots\ldots\ldots\ldots\ldots\ldots \text{(B-30)}$$

where

$$y = 54\theta_2'^8\theta_3'^2\sigma_{3i} + \frac{\sqrt{x}}{2} \ldots\ldots\ldots\ldots\ldots\ldots\ldots\ldots\ldots\ldots\ldots\ldots\ldots\ldots \text{(B-31)}$$

and

$$x = 11664\theta_2'^{16}\theta_3'^{4}\sigma_{2i}^2 + 864\theta_2'^{12}\theta_3'^{3}\left(\theta_3' - 2\theta_2'^{2}\sigma_{3i}^2\right)^3 \ldots\ldots\ldots\ldots\ldots\ldots\ldots\ldots\text{(B-32)}$$

In addition, if the imaginary part of those roots solutions is lower than or equal to 0.0001, the real part of the root is considered to be a solution.

APPENDIX C

**STEPWISE METHODOLOGY FOR FAILURE CRITERIA ESTIMATION
USING COMPUTER CODE**

Introduction

The objective of this appendix is to present the stepwise methodology to obtain the parametric representation of the failure criteria using the statistics-based method of error-in-variables (EIV). Fig. C-1 shows the five steps to be considered to derive the parametric solution of the failure criteria either in the plane or the space using a computer code. Short but clear explanations about each step are presented in this appendix.

Input Data

Typically, a failure criterion is expressed in terms of the major σ_1 and minor σ_3 principal stresses neglecting or ignoring the influence of the principal intermediate stress σ_2. If this is the case then the selected set of experimental data came out from a triaxial test. Then the input data is given by the axial and lateral stress measurements (σ_1, σ_3), which is represent by.

$$g(\sigma_1, \sigma_3) = 0 \dots\dots\dots\dots\dots\dots\dots\dots\dots\dots\dots\dots\dots\dots\dots\dots\dots\dots\dots\dots\dots\dots\dots\dots\text{(C-1)}$$

Because a failure criterion should exist not only in the compression region but also in the tensile region to be comprehensive enough the experimental data should contain tensile strength data, which is usually measured from a indirect tensile strength test like Brazilian Test. Considering the influence of poroelasticity and/or pore collapse
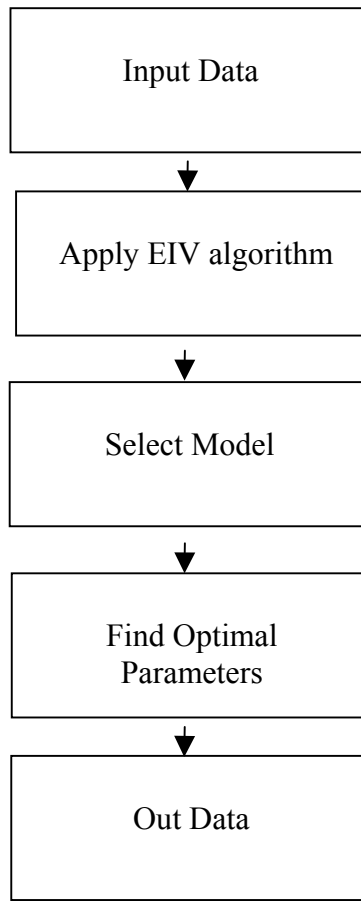
Fig. C-1- Stepwise methodology for failure criteria estimation using computer code.

to obtain the parametric representation of the failure envelope, the triaxial test experimental data should include pore pressure measurements for the input data.

If a three-dimensional failure criterion is proposed, its parametric representation can be expressed in terms of the minor, intermediate and major principal stresses. The experimental data use in 3D is obtained either from polyaxial or hollow cylinder test. In this case the input data is represented by.

$$g(\sigma_1, \sigma_2, \sigma_3) = 0 \quad \text{..} \quad \text{(C-2)}$$

Apply EIV algorithm

To obtain either the delimiting envelope or surface an appropriate algebraic form representing the failure criteria and a method of data fitting is needed. In our research the parametric representation of the failure surface can be obtained through the statistics-based method of error-in-variables that considers all the measured variables having experimental error. The presence of measurement errors in the system of variables is taken into account in the EIV approach, when formulating the objective function of the parameter estimation problem.

In the computer code we fit the experimental data to obtain the optimum parameters for the parametric representation of the failure criteria directly in the principal stress plane or space including or not pore pressure or in the Mohr plane using the corresponding EIV algorithm. Details about those algorithms were developed in Appendix A and B for fitting the failure criteria in 2D and 3D respectively.

In general, the EIV algorithm represents the concept of minimum distance between a measured point and the corrected or reconciled envelope or surface.

Select model

We can represent the failure criteria either in the stress-state plane or space to delimitate the boundary between stable and unstable conditions of the stress-state for the reservoir rock in the near-wellbore region.

If we neglect the influence of the intermediate principal stress, one of the most common ways to represent a failure criterion is using the Mohr plane. In such a case we can use either a linear model if we are interesting in a fast an accurate approximation or a nonlinear model when the problem demand more precision in obtaining the parametric representation of the failure envelope. Then the model can be expressed in implicit form as.

$$f(\hat{\sigma}, \hat{\tau}, \underline{\theta}) = 0 \dots\dots\dots\dots\dots\dots\dots\dots\dots\dots\dots\dots\dots\dots\dots\dots\dots (\text{C-3})$$

Another way is to plot the measured triaxial test data directly in the principal stress plane and with the statistics-based EIV method fit the failure envelope. Later on we can decide whether to perform a transformation process of the resulting envelope into the Mohr plane. To fit the measured data directly into the principal stress we can also use a linear and nonlinear model and its implicit form is as follow.

$$g(\hat{\sigma}_3, \hat{\sigma}_1, \theta') = 0 \dots\dots\dots\dots\dots\dots\dots\dots\dots\dots\dots\dots\dots\dots\dots (\text{C-4})$$

If the pore pressure measurement is considered to be important for the rock deformation behavior, which is the case of sedimentary rocks like sandstones that is the focus of our research, we must formulate the use of nonlinear model for an appropriate representation of the failure envelope in the principal-effective-stress plane.

$$h(\hat{\sigma}'_m, \hat{\sigma}_{eq}, \theta'') = 0 \dots\dots\dots\dots\dots\dots\dots\dots\dots\dots\dots\dots\dots (\text{C-5})$$

If we consider the influence of the principal intermediate stress with a system of variables σ_1, σ_2 and σ_3 the model can be written in implicit form as,

$$g(\hat{\sigma}_1, \hat{\sigma}_2, \hat{\sigma}_3, \theta') = 0 \ \text{..} \ \text{(C-6)}$$

Select an appropriate algebraic form to represent the failure criteria either in 2D and 3D is needed. In Appendix A and B we present the derived equations for each of the proposed models.

Find optimal parameters

Appling the corresponding EIV algorithms to the select model, we can reconcile the measured points to the failure envelope or surface using the concept of the shortest distance. The optimal parameters of the failure envelope can be obtained through minimizing the objective function, which is nothing but to minimize the sum of square distance.

When the EIV method of curve fitting is apply directly in the Mohr plane. The corresponding sum of squared distance is given by.

$$J = \sum_{i=1}^{n} \left(\sqrt{(c_i - \hat{\sigma}_i)^2 + \hat{\tau}_i^2} - r_i \right)^2 \ \text{..}\text{(C-7)}$$

If we propose to fit the failure envelope directly from the raw data into the principal-stress plane the sum of squared distance is given by.

$$J = \sum_{i=1}^{n} \left((\hat{\sigma}_{3i} - \sigma_{3i})^2 + (\hat{\sigma}_{1i} - \sigma_{1i})^2 \right)^2 \ \text{..}\text{(C-8)}$$

Introducing pore pressure effect to obtain the failure or yield envelope to consider the brittle/ductile region of rock deformation, the sum of square distance is given by.

$$J = \sum_{i=1}^{n} \left((\hat{\sigma}'_{mi} - \sigma'_{mi})^2 + (\hat{\sigma}_{eqi} - \sigma_{eqi})^2 \right)^2 \ \text{..}\text{(C-9)}$$

When the influence of the principal intermediate stress is consider in the system of variables the sum of square distance can be written as,

$$J = \sum_{i=1}^{n} \left((\hat{\sigma}_{3i} - \sigma_{3i})^2 + (\hat{\sigma}_{2i} - \sigma_{2i})^2 + (\hat{\sigma}_{1i} - \sigma_{1i})^2 \right)^2 \quad \dots\dots\dots\dots\dots\dots\dots\dots\dots\dots (C\text{-}10)$$

Output data

Once the optimum parameters of the envelope or surface have been obtained by applying the corresponding EIV algorithms to the select model to reconcile the measured or derived points, the resulting parameters can be used to construct a group of plot and tables to show up the optimal parametric representation of the failure criteria. Tables and figures with the different results obtained in our research after applying the EIV method of curve fitting are showed up in the main body of this fundamental research work.

VITA

Name: ORLANDO ZAMBRANO MENDOZA

Born: January 10, 1963

Permanent address: Harold Vance Department of Petroleum Engineering, Texas A&M University, College Station, Texas.

Education: Zulia University (Venezuela), B.S., Petroleum Engineering, 1991
                                   Zulia University (Venezuela), M.S., Petroleum Engineering, 1998
                                   Texas A&M University (USA), Ph.D., Petroleum Engineering, 2004

Experience: Production Technology, Drilling and Work over, PDVSA, Venezuela, 1990-1992
                                   Professor (Drilling and Work over), Zulia University, Venezuela, 1992-1998

Professional Society: Society of Petroleum Engineers (since 1999)